

Metallurgical Characteristics of High Strength Structural Materials

Eleventh Quarterly Report

P. P. PUZAK, K. B. LLOYD, R. W. HUBER,
R. J. GOODE, E. A. LANGE, C. N. FREED, T. W. CROOKER,
R. W. JUDY, JR., AND D. G. HOWE

Metallurgy Division

August 1966



NAVAL RESEARCH LABORATORY
Washington, D.C.

DISTRIBUTION OF THIS DOCUMENT IS UNLIMITED

PREVIOUS REPORTS IN THIS SERIES

First Quarterly Report - "Metallurgical Characteristics of High Strength Structural Materials," P.P. Puzak, K.B. Lloyd, E.A. Lange, R.J. Goode, R.W. Huber, E.P. Dahlberg and C.D. Beachem, NRL Memo Report 1438, June 30, 1963

Second Quarterly Report - "Metallurgical Characteristics of High Strength Structural Materials," P.P. Puzak, K.B. Lloyd, E.A. Lange, R.J. Goode, and R.W. Huber, NRL Memo Report 1461, September 1963

Third Quarterly Report - "Metallurgical Characteristics of High Strength Structural Materials," P.P. Puzak, K.B. Lloyd, R.J. Goode, R.W. Huber, D.G. Howe, T.W. Crooker, E.A. Lange, and W.S. Pellini, NRL Report 6086, January 1964

Fourth Quarterly Report - "Metallurgical Characteristics of High Strength Structural Materials," R.J. Goode, R.W. Huber, D.G. Howe, R.W. Judy, Jr., T.W. Crooker, R.E. Morey, E.A. Lange, P.P. Puzak, and K.B. Lloyd, NRL Report 6137, June 1964

Fifth Quarterly Report - "Metallurgical Characteristics of High Strength Structural Materials," T.W. Crooker, R.E. Morey, E.A. Lange, R.W. Judy, Jr., C.N. Freed, R.J. Goode, P.P. Puzak, K.B. Lloyd, R.W. Huber, D.G. Howe, and W.S. Pellini, NRL Report 6196, September 1964

Sixth Quarterly Report - "Metallurgical Characteristics of High Strength Structural Materials," W.S. Pellini, R.J. Goode, R.W. Huber, D.G. Howe, R.W. Judy, Jr., P.P. Puzak, K.B. Lloyd, E.A. Lange, E.A. DeFelice, T.W. Crooker, R.E. Morey, E.J. Chapin, and L.J. McGeady, NRL Report 6258, December 1964

Seventh Quarterly Report - "Metallurgical Characteristics of High Strength Structural Materials," R.J. Goode, D.G. Howe, R.W. Huber, P.P. Puzak, K.B. Lloyd, T.W. Crooker, R.E. Morey, E.A. Lange, R.W. Judy, Jr., and C.N. Freed, NRL Report 6327, May 1965

Eighth Quarterly Report - "Metallurgical Characteristics of High Strength Structural Materials," P.P. Puzak, K.B. Lloyd, R.J. Goode, R.W. Huber, D.G. Howe, R.W. Judy, Jr., T.W. Crooker, R.E. Morey, E.A. Lange, and C.N. Freed, NRL Report 6364, August 1965

Ninth Quarterly Report - "Metallurgical Characteristics of High Strength Structural Materials," R.J. Goode, R.W. Huber, D.G. Howe, R.W. Judy, Jr., P.P. Puzak, K.B. Lloyd, T.W. Crooker, R.E. Morey, E.A. Lange, and C.N. Freed, NRL Report 6405, November 1965

Tenth Quarterly Report - "Metallurgical Characteristics of High Strength Structural Materials," R.J. Goode, R.W. Huber, R.W. Judy, Jr., D.G. Howe, P.P. Puzak, K.B. Lloyd, T.W. Crooker, R.E. Morey, E.A. Lange, and C.N. Freed, NRL Report 6454, April 1966

CONTENTS

| | |
|--|-----|
| Abstract | iii |
| Problem Status | iii |
| Authorization. | iii |
| INTRODUCTION | 1 |
| FRACTURE TOUGHNESS CHARACTERISTICS OF HIGH STRENGTH STEELS. | 3 |
| The Fracture Toughness Index Diagram for Steels. | 4 |
| Welding Studies | 6 |
| Fracture Toughness Characterization of a Special Melt Practice 250 ksi Yield Strength Maraging Steel | 15 |
| Fracture Toughness Characterization of a Special Melt Practice Cr-Ni-Mo Precipi- tation Hardening Stainless Steel. | 18 |
| FRACTURE TOUGHNESS CHARACTERISTICS OF TITANIUM ALLOYS | 23 |
| Recent Fracture Toughness Studies | 25 |
| 2000 FT-LB SHOCKLESS TEAR TEST MACHINE | 27 |
| PLANE STRAIN FRACTURE TOUGHNESS TESTING OF TITANIUM AND ALUMINUM ALLOYS | 31 |
| Experimental Details and Materials. | 32 |
| K_{Ic} Data for Four Aluminum Alloys | 34 |
| K_{Ic} Data for Two Titanium Alloys. | 36 |
| Correlation of β_{Ic} with DWTT and Yield Stress with K_{Ic} | 38 |
| LOW CYCLE FATIGUE CRACK PROPAGATION IN 9Ni-4Co-0.25C STEEL IN AIR AND 3.5 PERCENT SALT WATER. | 41 |

CONTENTS (Continued)

| | |
|---|----|
| Test Material | 42 |
| Results and Discussion. | 44 |
| Evaluation and Conclusions. | 47 |
| STRESS CORROSION CRACKING STUDIES OF SOME HIGH STRENGTH METALS. | 49 |
| SCC of Some Titanium Alloys | 50 |
| Short-Term SCC of HY-130/150 Plate and a 9Ni-4Co-0.25C Weldment. | 61 |
| SCC of Aluminum Alloys. | 71 |
| HEAT-TREATMENT STUDIES | 71 |
| REFERENCES | 75 |

ABSTRACT

A progress report covering the research studies in high strength structural metals conducted during the period April through June 1966 is presented. The report includes fracture toughness studies on specially melted 18% Ni grade 250 ksi maraging steel and a Cr-Ni-Mo stainless steel. Welding studies on a 12Ni-5Cr-3Mo maraging steel with 12Ni-3Cr-3Mo and 17Ni-2Co-3Mo filler metal wire are described with the problems associated with developing optimum properties in both plate and weldment being discussed. Results of fracture toughness studies on titanium alloys and aluminum alloys are presented in which engineering type tests and fracture mechanics techniques are employed. The fracture toughness index diagrams for steels and titanium are presented based upon the correlations developed with the engineering test methods. Preliminary fracture toughness correlation diagrams are presented for titanium alloys based upon fracture mechanics test methods. Results of a study on the low cycle fatigue crack propagation of a 9Ni-4Co-0.25C steel in air and salt water is discussed and compared to similar data obtained for other steels covering a spectrum of yield strengths. Stress-corrosion-cracking studies were conducted on titanium alloys, aluminum alloys, and steels. The stress-corrosion-cracking resistance of these alloys is presented in terms of the stress intensity (K_{ISCC}) required to cause crack propagation to occur due to the influence of the environment. A double-pendulum type, shock-free, 2000 ft-lb impact machine has been designed to obtain fracture appearance, tear energy, and dynamic K_{IC} information on high strength structural metals using a subsized tear type specimen. Design details of this new test tool are presented.

PROBLEM STATUS

This is a progress report; work is continuing.

AUTHORIZATION

NRL Problem F01-17; Project SP-01426.
NRL Problem M01-05; Projects RR-007-01-46--5405,
SF-020-01-01-0724, and SP-01426.
NRL Problem M01-18; Projects RR-007-01-46--5420,
SF-020-01-05--0731, SP-01426,
and ENG-NAV-66-2.
NRL Problem M03-01; Projects RR-007-01-46--5414,
SF-020-01-01--0850, and SP-01426.
NRL Problem M04-08B; ARPA 878.

Manuscript submitted November 10, 1966.

METALLURGICAL CHARACTERISTICS OF
HIGH STRENGTH STRUCTURAL MATERIALS

[Eleventh Quarterly Report]

INTRODUCTION

This report is the eleventh in the series of status reports covering the Naval Research Laboratory Metallurgy Division's long-range Advanced High Strength Structural Metals Program. This program is concerned with determining the performance characteristics of high strength metals and is directed at developing the necessary information to provide "guideline" principles for the metallurgical optimization of alloys, for processing and fabrication techniques, and for reliable failure-safe utilization of these materials in large complex structures. Fracture toughness aspects of the failure-safe design problem are being studied with recently developed and conventional, long-established engineering test methods. The subcritical crack growth characteristics of the high strength metals are studied under conditions of low cycle fatigue. Environmental effects on subcritical crack growth and the application of fracture mechanics techniques for the spectrum of material under investigation are also being studied.

The Charpy V-notch (for steels), drop-weight tear, and explosion tear tests have been used to determine the fracture toughness characteristics of steels, titanium alloys, and aluminum alloys over wide ranges of yield strengths and have made possible the development of preliminary fracture toughness index diagrams for these materials. The diagrams provide guideline information for purposes of design, alloy development, specification, and quality control. The latest diagrams for steels and titanium alloys are presented in this report.

Welding studies on 2-in.-thick 12Ni-5Cr-3Mo maraging steel plate are described in which 12Ni-3Cr-3Mo and 17Ni-2Co-3Mo filler metal compositions were used. Generally, the weldments with the 12Ni-3Cr-3Mo wire had higher fracture toughness and lower yield strength values than those with the 17Ni-2Co-3Mo wire for comparable welding conditions. Development of optimum toughness-strength conditions in the

weld required different aging temperatures and times than that required for the base plate. This indicates a potential compatibility problem of these weld metal compositions with the 12Ni-5Cr-3Mo maraging steel. Fracture toughness characterization studies as a function of heat treatment were conducted on a vacuum induction melted-vacuum arc remelt 18% Ni grade 250 ksi yield strength maraging steel and a similarly melted experimental Cr-Ni-Mo precipitation hardening stainless steel. The 18% Ni maraging steel had low levels of fracture toughness in the yield strength range of 220 to 280 ksi for all heat treatments investigated. The Cr-Ni-Mo stainless steel displayed a sizeable variation of through-thickness properties in the fracture toughness tests.

Preliminary results of fracture toughness studies on Ti-6Al-2Cb-1Ta-0.8Mo, which includes a study on the effects of processing on fracture toughness for this alloy as well as for a Ti-6Al-4V alloy, are presented. The properties developed by the Ti-6Al-4V alloy exceed the established optimum materials trend line for titanium alloys. Drop-weight tear test results are presented for a preliminary study on a number of 2-in.-thick titanium alloy plates.

A 2000 ft-lb double-pendulum type impact machine has been designed and built for use with the subsized tear specimen for providing dynamic K_{Ic} , fracture appearance, and tear energy data. The machine is designed to provide for a minimum of shock transmission for future use in the study of irradiation damage effects in high strength metals in a hot-cell facility. The design features and characteristics of this new test tool are described.

The results of plane strain fracture toughness studies on titanium and aluminum alloys using single-edge-notch and notch-bend specimens of 1-in.-thick plate material are presented. The aluminum alloys 2020, 2219-T851, 7079-T6, and 7106-T63 were studied in the as-received condition and the titanium alloys Ti-6Al-4Zr-2Mo and Ti-6Al-4V-2Sn were studied in various heat-treated conditions. The plane strain fracture toughness data obtained to date for titanium alloys have been correlated with drop-weight tear test energy measurements. The fracture mechanics data in this correlation are expressed in the terms β_{Ic} which provides an indication of the characteristic dimension of the plastic zone size:

$$\beta_{Ic} = \left[\left(\frac{K_{Ic}}{\sigma_{ys}} \right)^2 \frac{1}{B} \right]$$

The plane strain fracture toughness K_{IC} is also correlated to yield strength providing preliminary information concerning the optimum levels of plane strain fracture toughness for different levels of yield strength for the titanium alloys.

Low cycle fatigue studies on a 9Ni-4Co-0.25C steel in air and in 3.5 percent salt water are described in which it is found that the crack propagation rate as a function of total strain range follows a power-law relationship to the 6th power. This indicates that the crack propagation rate is highly sensitive to small changes in the level of cyclic strain in air. The fatigue crack growth rate is increased by more than an order of magnitude at low levels of total strain range in the salt water solution, but at high levels of total strain range, converge with the air data. The data are compared to those obtained for other steels covering a wide range of yield strengths.

The aqueous stress-corrosion-cracking resistances of a number of titanium alloys, aluminum alloys, and steels have been determined using the cantilever bend test. Also, preliminary data on the effects of heat treatment in vacuum and argon are presented for several titanium alloys which show that vacuum heat treatments essentially eliminate environmental sensitivity in the alloys.

FRACTURE TOUGHNESS CHARACTERISTICS OF HIGH STRENGTH STEELS

(P.P. Puzak & K.B. Lloyd)

Continuing investigations to determine the performance characteristics of high strength steels and welds are aimed at developing the necessary information to provide "guideline" principles for the metallurgical optimization of alloys, processing and fabrication techniques, and the reliable failure-safe utilization of steels in large, complex, welded structures. The principal fracture toughness test employed in these studies has been the drop-weight tear test (DWTT) as correlated with results obtained in the large structural prototype element explosion tear test (ETT). These tests and the correlation procedure have previously been described in detail in Ref. (1). From these studies, a simplified Fracture Toughness Index Diagram (FTID) which indexes the DWTT fracture toughness characteristics of the steel in terms of the ETT performance of the material has been evolved. Interpretation of the FTID data

is aimed at providing more definitive information relative to the fracture-safe design utilization of the high strength steels in thick sections of complex welded structures.

THE FRACTURE TOUGHNESS INDEX DIAGRAM FOR STEELS

The FTID for 1-in.-thick high strength steels is shown in Fig. 1. This diagram has been updated to present the latest information. The "fracture-index" aspects of the diagram are illustrated by the horizontal crosshatched lines and shaded region on the left side of the FTID. These depict the significance of the DWTT energy values presently established by indexing them to the ETT performance of the steels. For example, steels having DWTT energy values below the 1000-1250 ft-lb range shown by the shaded region have been characterized by the "flat breaks" and shattering in the ETT and thus would be expected to propagate fractures at elastic stress levels. Above the 1000-1250 ft-lb DWTT energy range, the relative level of DWTT energy is proportional to the expected level of plastic strain overload required to propagate a fracture in the ETT as shown by the strain level values indicated above, between, or below the horizontal crosshatched lines given on the left side of the FTID. Each of the curves in this figure is designated an optimum materials trend line (OMTL) which separates the data into characteristic groups relating to the mill processing variables (melting practice and/or cross-rolling) of the steels. All steel data relating to the limiting ceiling OMTL curve for special melt practice steels have involved vacuum-induction-melt (VIM) or a double vacuum practice of VIM plus vacuum-arc-remelt (VIM + VAR). To date, material produced by VIM or VIM + VAR practices have appeared to develop superior toughness properties than the steels of similar composition melted by other means using less exacting controls. The fact that the DWTT energy values for many of the steels within a characteristic grouping are not close to the OMTL is indicative of either poor chemistry, non-optimized processing, or heat treatment, or a combination of these conditions. Evaluation of additional VIM and VIM + VAR practice steels capable of developing yield strength (YS) levels in excess of 200 ksi are required for better definition of the dashed portion of the presently depicted limiting ceiling OMTL curve.

The primary evaluation criterion for suitability of materials in complex welded structures is provided by the elastic-to-plastic performance transition band (1000-1250 ft-lb shaded

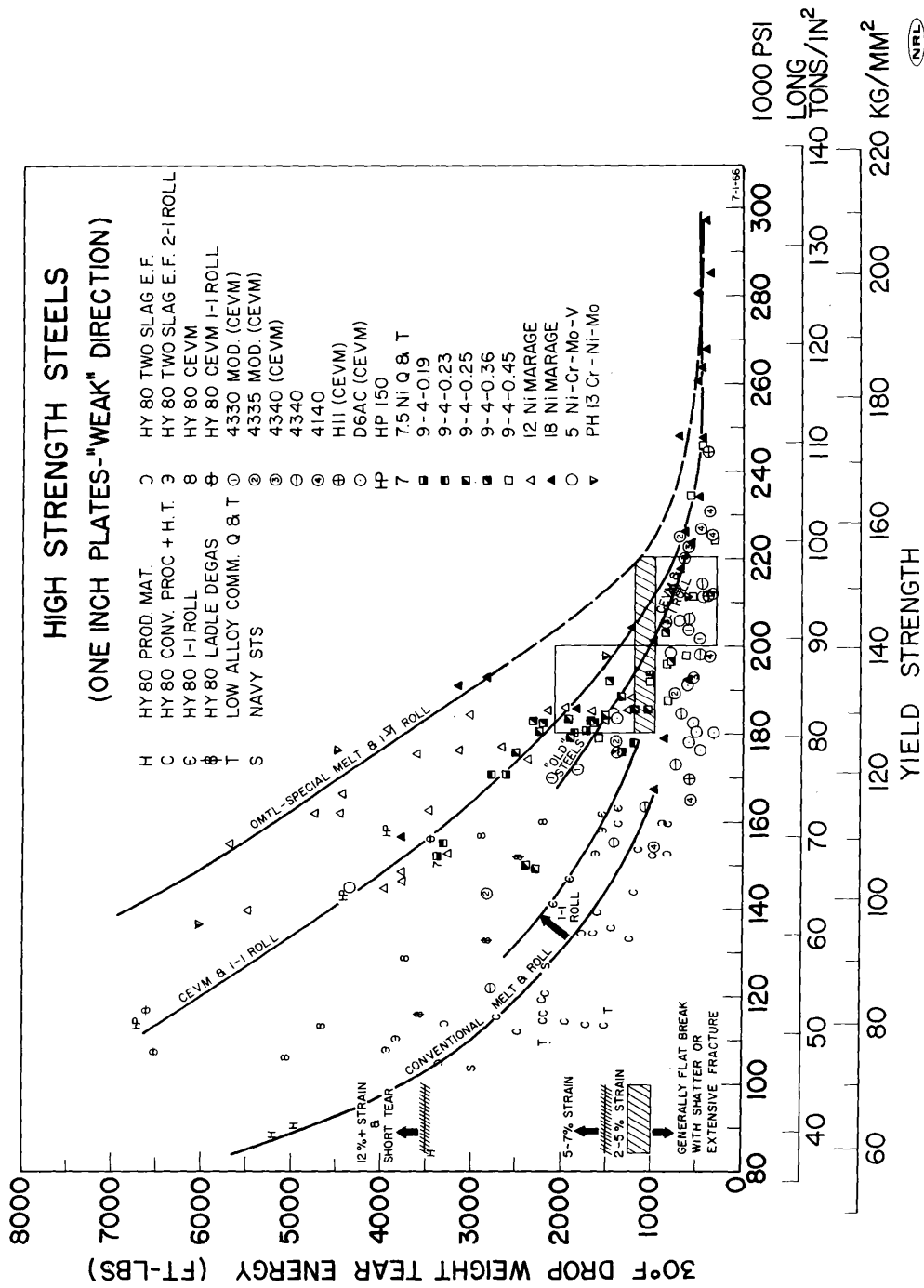


Fig. 1 - Fracture Toughness Index Diagram derived from all high strength steels tested. The ETT Correlation and the OMTL for various mill practices are included.

region in Fig. 1) of the FTID. Consideration of new alloys, or special processing, would be required to improve the fracture toughness of any characteristic group of steels at strengths higher than the maximum YS level at which the various OMTL curves cross over this transition band. For example, the cross over of the OMTL for the "best" presently defined alloy steels indicates that all steels above about 200-210 ksi YS for CEVM (consumable electrode vacuum melt) practice and about 200-230 ksi YS for special melt VIM practice are of low fracture toughness and should be expected to propagate fractures through elastic stress regions. Fracture mechanics techniques will be required to adequately determine the fracture toughness characteristics of these steels. For the steels of high fracture toughness levels (plastic strains required for fracture propagation), it is considered that the DWTT energy value provides a more significant indication of toughness per se than might be apparent from a "lower-bound" fracture mechanics evaluation.

A surprisingly good correlation of the DWTT and Charpy V (C_V) energy values has been developed for the steels providing that only maximum C_V (upper shelf, 100% shear fractures) energy levels are considered. Within this limitation, the DWTT correlations and ETT index procedures have been used to evolve the FTID in terms of C_V -YS data given in Fig. 2 for all 1-in.-thick steel plates tested to date. Generally the illustrated OMTL curves in this figure separate these data into characteristic groups relating to the process variables of the steels similar to those shown in Fig. 1. Wherever possible, new data (to be described) are reported in charts containing the basic curves and correlation features of the FTID to provide a ready comparison with data previously reported.

WELDING STUDIES

A new precision-built, fully-automatic MIG-TIG fusion welding equipment and controls package (600 amp direct current, three-phase, full-wave rectifier type, constant current or constant potential output welding power source, main console and operator controls, and 10-ft-long side-beam track and carriage) was procured and installed at the end of the previous reporting period. The equipment is now fully operational and data for weldments fabricated with this new welding facility are expected to be developed during the next reporting period.

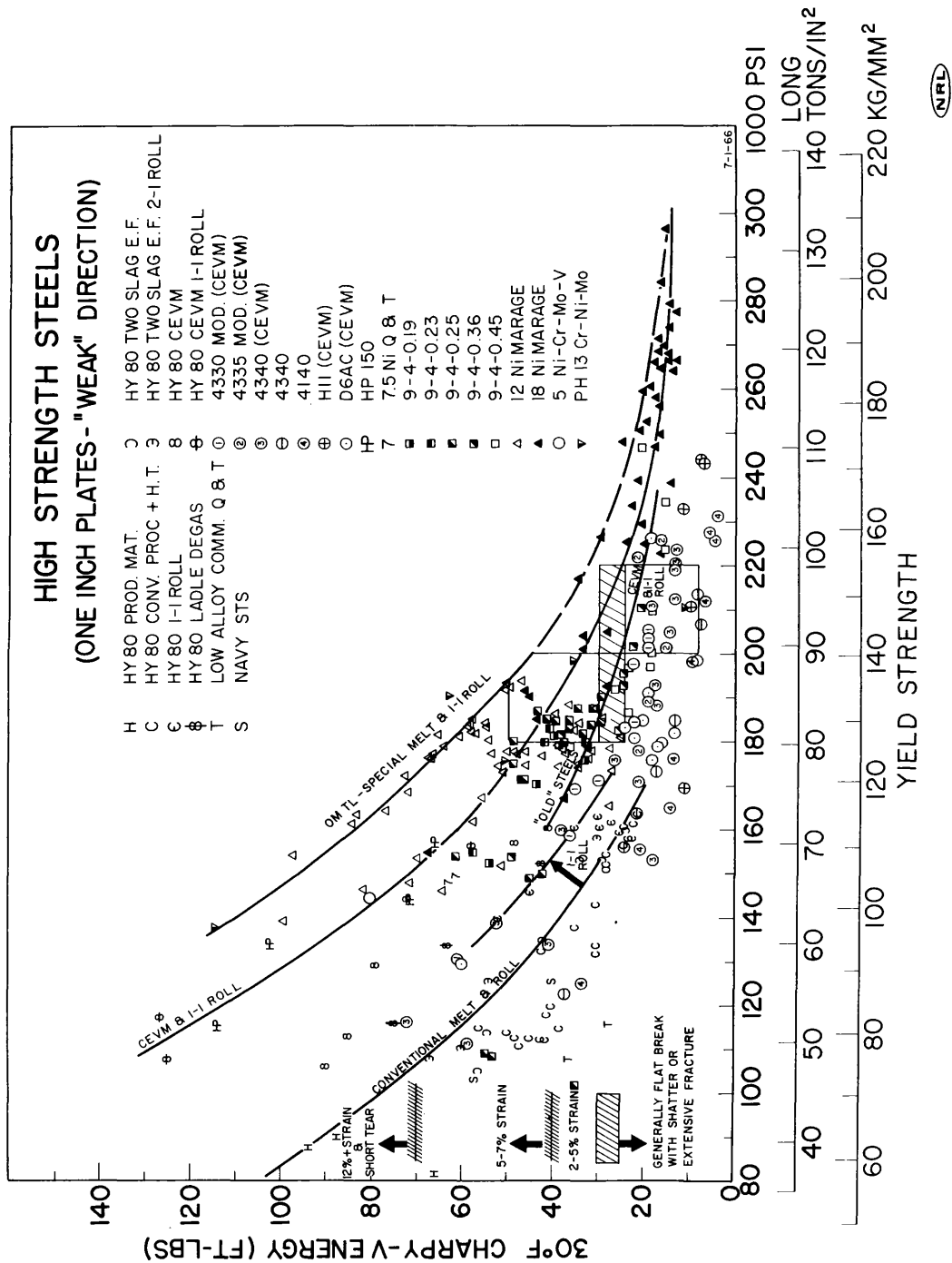


Fig. 2 - Summary of Charpy V data for high strength steels as a function of YS. The OMTL for various mill practices show same trends as Fig. 1.



During the instructional and familiarization period of the operator with this automatic welding equipment, considerable difficulties were encountered in controlling weld metal porosity. These were generally corrected by modifications in welding procedures (electrode size, inert-gas coverage, arc length, etc.) and X-ray examination; crystal clear weldments are now produced consistently by the operator. A weld and plate metal cracking problem was encountered in one weldment of a 12Ni-5Cr-3Mo (12-5-3) maraging steel fabricated during this period which could not be attributed to procedure or operator difficulties. This weld was being made in a fully annealed and aged section of a 2-in.-thick 12-5-3 plate (No. J1) which comprised material remaining from one of the high purity, VIM practice maraging steels previously evaluated by NRL (2). The plate metal cracking observed was of the type termed "delamination cracks" resulting from the presence of continuous or semicontinuous internal layers of nonmetallic inclusions. Discussion of this cracking problem with producer's representatives disclosed the fact that similar cracking had been observed in weldments of other plates from this heat of 12-5-3 maraging steel. In all cases, the nonmetallic "dirt" was found in plates produced only from the bottom of the ingot. The VIM process employed to produce these plates is not amenable to bottom pouring, and the condition was considered attributable to the entrapment of slag and other nonmetallics during the lip-pouring of the ingot. This potential problem emphasizes the need for reliable non-destructive testing techniques for acceptance purposes to insure the quality and soundness of the plate product.

As described in earlier reports (2-4), two weld metals have been evolved for fabricating the new 12-5-3 maraging steels. These comprise a nominal 12Ni-3Cr-3Mo (12-3-3) wire composition, expected to develop a 160 ksi minimum YS upon aging, and a nominal 17Ni-2Co-3Mo (17-2-3) wire composition, expected to develop a 180 ksi minimum YS upon aging. Limited preliminary evaluations of producer-fabricated, automatic TIG process weldments using experimental electrodes of both compositions produced from small (30 to 150 lb) research quality heats were generally encouraging with respect to performance in explosion bulge and drop-weight tear tests (3,4). Weld wire representative of semiproduction heats (product from 1000-lb melts) of both nominal 12-3-3 and 17-2-3 compositions have been procured for this investigation. Initial studies with

these weld metals have been aimed at determining optimum aging treatment conditions necessary to develop the best combination of strength and toughness properties in welds deposited under a variety of conditions. Appropriately optimized 1- to 2-in.-thick weldments of these and other high strength materials are to be produced to meet the test and investigation requirements of plane strain fracture mechanics (K_{IC}) and engineering methods (DWTT, C_V , etc.) fracture toughness determinations, stress-corrosion-cracking, and fatigue (strain range basis) crack propagation rate studies.

Prior to the fabrication of the relatively large (18- to 30-in. transweld dimension) weldments required for this program, initial exploratory weldments required for optimization studies of a given weld metal involves the use of small remnant pieces of plate material remaining from the steels previously evaluated. These smaller weldments are generally cut into small blocks (5-in. length x 2 1/4-in. transweld) which are appropriately heat treated and then sectioned to provide material for one all-weld-metal 0.505-in.-diam tensile test specimen and usually 10 C_V test specimens per each heat treatment condition. In an earlier report (4), exploratory data were described for manual TIG welds made with heat input energies of approximately 40,000 to 45,000 joules/inch. Three strands of the 1/16-in.-diam wire were twisted to form a suitable filler wire for manual TIG welding and a relatively large number of small weld bead passes (approximately 85 to 90 passes for 2-in.-thick welds) were required to complete the welds. Additional manual TIG weldments with the 17-2-3 filler wire have been evaluated similarly to that described above. However, approximately 60,000 to 65,000 joules/inch heat input was used which reduced by about one-half the number of weld passes required. The summary of new data is given in Table 1 and depicted graphically in Fig. 3, as referenced to the FTID for 1-in.-thick steel plates. The shaded region in this illustration represents the data band established previously (1) for automatic TIG welds using experimental electrodes produced from small heats of material and used to fabricate 1/2-in.-thick weldments. Generally it is noted that these "high" heat input welds of the 17-2-3 filler wire composition are characterized by considerably lower C_V toughness values than those denoted by the shaded band for the small-heat, experimental wire compositions.

TABLE 1
 CHARPY V AND TENSILE TEST DATA
 AGED 17-2-3 WIRE--MANUAL TIG WELDS*

| Aging Temp. (°F) | Aging Time (hr) | 0.505-in.-diam Tensile Test Data All Weld Metal Specimens | | | | Transverse Weld Charpy V | |
|------------------|-----------------|--|-----------|---------------|--------|--------------------------|---------|
| | | 0.2% YS (ksi) | UTS (ksi) | El. in 2" (%) | RA (%) | at 30°F | at 80°F |
| 800 | 1 | 146.2 | 155.6 | 17.0 | 59.2 | 48 | 50 |
| 800 | 3 | 152.8 | 164.4 | 14.0 | 53.0 | 36 | 37 |
| 800 | 10 | 169.2 | 179.3 | 13.0 | 49.8 | 33 | 34 |
| 800 | 24 | 177.7 | 185.4 | 13.0 | 53.0 | 34 | 37 |
| 825 | 1 | 154.9 | 162.5 | 15.5 | 54.0 | 44 | 46 |
| 825 | 3 | 164.9 | 172.4 | 13.0 | 52.0 | 31 | 36 |
| 825 | 10 | 173.6 | 180.4 | 12.0 | 50.5 | 31 | 29 |
| 825 | 24 | 180.1 | 187.7 | 14.0 | 50.7 | 34 | 34 |
| 850 | 1 | 162.3 | 168.2 | 15.0 | 58.2 | 33 | 33 |
| 850 | 3 | 172.1 | 178.1 | 13.5 | 53.7 | 31 | 36 |
| 850 | 10 | 179.4 | 185.8 | 12.0 | 45.0 | 26 | 28 |
| 850 | 24 | 179.3 | 186.2 | 12.0 | 51.2 | 32 | 33 |
| 875 | 1 | 164.2 | 172.9 | 13.0 | 46.8 | 31 | 35 |
| 875 | 3 | 171.8 | 181.3 | 14.5 | 55.7 | 29 | 32 |
| 875 | 10 | 175.4 | 183.6 | 17.5 | 50.7 | 25 | 26 |
| 900 | 1 | 166.5 | 174.5 | 14.0 | 52.2 | 26 | 31 |
| 900 | 3 | 172.0 | 179.8 | 13.3 | 61.0 | 30 | 31 |
| 900 | 10 | 174.0 | 181.7 | 14.0 | 55.0 | 32 | 29 |

* All welds made in 1 1/2-in.-thick, VV joint, 12-5-3 maraging steel plate.

Also, the C_V energy values of the high heat input welds were slightly lower than those of the 17-2-3 wire composition made earlier using the low heat input condition.

Additional high heat input weldments were made with the 12-3-3 filler wire composition and evaluated as described above. Table 2 provides a summary of these data and Fig. 4 depicts graphically the observed C_V -YS relationships as referenced to the FTID for 1-in.-thick steel plate. Generally the 12-3-3 filler wire welds exhibit considerably higher C_V toughness values and lower YS values than those of the 17-2-3 filler wire welds for comparable welding conditions. Of particular significance, however, is that both of these weld compositions are noted to develop optimum toughness-strength relationships upon aging for relatively long times (10 to 24 hours) at approximately 850°F, and that short time aging (1 to 3 hours) at 900°F results in the development of YS levels 15 to 20 ksi below the 160 and 180 ksi YS "expected" respectively for the 12-3-3 and 17-2-3 weld metals. This response of these weld metals to the aging heat treatments raises some questions as to whether these weld compositions should be considered fully compatible with the 12-5-3 plate alloy which normally is expected to develop 180 ksi YS upon aging at 900°F for only 3 hours. Ideally, both the maraging steel plate and the weld should develop equivalent toughness and YS levels upon aging for the same time at the same temperature. The necessity for aging the weld metal at different temperatures or times from those known to develop optimum plate metal properties introduces the possibility of producing severely mismatching weldments with respect to weld and plate metal YS. Studies are underway at the International Nickel Co. Research Laboratory which are aimed at evolving new weld metal compositions that will essentially be fully compatible in YS and toughness properties to those developed by the 12-5-3 maraging steel plate alloy for any given aging heat treatment. Continuing weldment evaluation studies in this program are expected to explore the effects of long-time aging at 850°F on the available 12-5-3 plate alloys and to establish weld metal properties of weldments fabricated with low heat input (20,000 to 40,000 joules/inch) and small weld bead passes which appear to be most favorable for development of optimum toughness in the now available 12-3-3 and 17-2-3 maraging steel weld metal compositions.

TABLE 2
 CHARPY V AND TENSILE TEST DATA
 AGED 12-3-3 WIRE--MANUAL TIG WELDS

| Aging Temp. (°F) | Aging Time (hr) | 0.505-in.-diam Tensile Test Data All Weld Metal Specimens | | | | Transverse Weld Charpy V | |
|------------------|-----------------|--|-----------|---------------|--------|--------------------------|---------|
| | | 0.2% YS (ksi) | UTS (ksi) | El. in 2" (%) | RA (%) | at 30°F | at 80°F |
| 850* | 1 | 135.7 | 139.4 | 19.0 | 38.1 | 66 | 71 |
| 850* | 3 | 146.3 | 150.7 | 13.0 | 42.8 | 67 | 73 |
| 850 | 10 | 160.6 | 164.3 | 14.5 | 55.7 | 41 | 43 |
| 850 | 24 | 161.8 | 166.4 | 16.5 | 62.3 | 48 | 48 |
| 875* | 1 | 139.2 | 144.7 | 17.0 | 58.7 | 60 | 72 |
| 875* | 3 | 147.6 | 152.1 | 17.0 | 60.9 | 70 | 70 |
| 875* | 10 | 149.0 | 153.0 | 16.0 | 57.2 | 65 | 72 |
| 875 | 24 | 163.4 | 167.7 | 14.0 | 52.7 | 50 | 47 |
| 900* | 1 | 145.1 | 148.1 | 16.5 | 56.2 | 71 | 70 |
| 900* | 3 | 149.9 | 153.2 | 14.5 | 44.3 | 62 | 66 |
| 900* | 10 | 150.1 | 152.9 | 11.0 | 36.3 | 59 | 59 |
| 900 | 24 | 159.8 | 165.6 | 16.0 | 57.4 | 45 | 49 |
| 925 | 1 | 154.2 | 159.2 | 15.0 | 59.7 | 44 | 46 |
| 925 | 3 | 158.3 | 163.0 | 16.0 | 63.3 | 48 | 43 |
| 925 | 10 | 159.5 | 164.1 | 14.5 | 50.7 | 56 | 56 |
| 925 | 24 | 158.6 | 166.7 | 17.0 | 56.2 | 59 | 60 |
| 950 | 1 | 151.3 | 155.2 | 16.0 | 59.4 | 59 | 53 |
| 950 | 3 | 153.4 | 157.4 | 13.5 | 45.3 | 50 | 55 |
| 950 | 10 | 153.9 | 160.1 | 17.5 | 61.9 | 68 | 66 |
| 950 | 24 | 156.9 | 166.3 | 15.5 | 50.2 | 48 | 53 |

* Welds made in 2-in.-thick plate; all others made in 1 1/2-in.-thick, VV joint, 12-5-3 maraging steel plate.

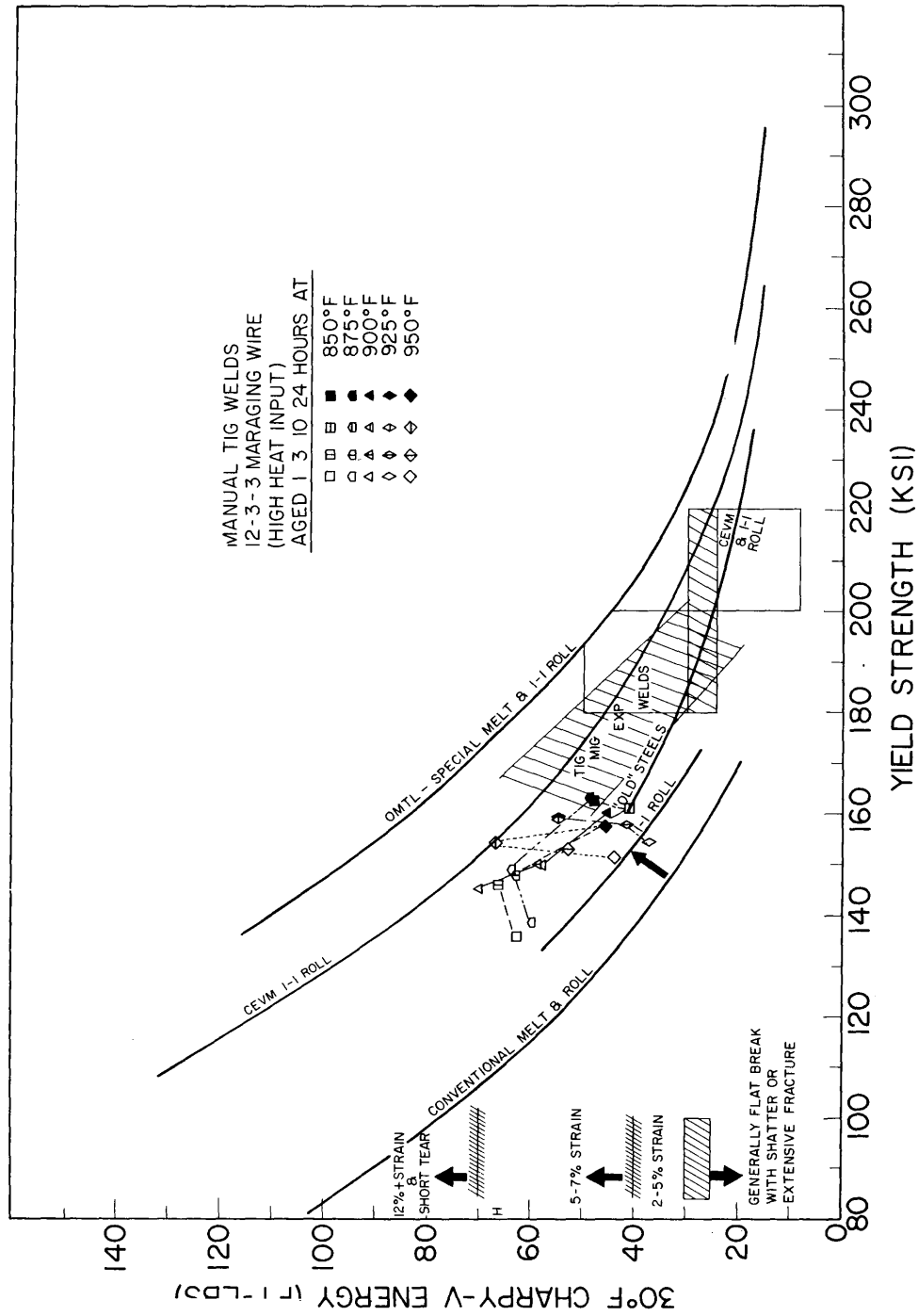


Fig. 4 - Summary of Charpy V energy value YS relationships of high heat input manual TIG welds with a nominal 12Ni-3Cr-3Mo wire composition maraging steel.

FRACTURE TOUGHNESS CHARACTERIZATION OF A SPECIAL MELT PRACTICE 250 KSI YIELD STRENGTH MARAGING STEEL

Drop-weight tear test and heat-treatment studies of a VIM + VAR, controlled chemistry (low carbon, manganese, silicon, and sulphur) 18% Ni grade 250 ksi YS maraging steel have been completed. The 1-in.-thick plate had been rolled from heavier gage (4-in.) plate especially produced for a joint Carpenter Steel Co.-Lukens Steel Co. research and development program to study the effects of controlled chemistry on banding and mechanical properties in heavy sections of the standard grade material. Generally, the results reported in this cooperative research program indicated this VIM + VAR steel to be definitely superior, with particularly high DWTT values for through-gage tests that ranked it above any previous experience for large commercial heats in heavy plate form (5).

The 1-in.-thick plate (No. J16) was received in the mill-solution-annealed (1650°F) condition. Drop-weight tear test specimens were cut and aged at 900°F for 3 hours which resulted in developing a 248 ksi YS level. The average DWTT energy required to fracture the J16 specimens was 730 ft-lb. Even though the very best of melting practices and exacting control of chemical composition employed for this 250 ksi YS maraging steel did not raise its level of fracture toughness out of the fracture mechanics regions, the 730 ft-lb DWTT energy value is the highest value observed to date for any high strength steel of about 230 to 300 ksi YS.

In heat-treatment studies conducted with a 12% Ni maraging steel, significant improvements in fracture toughness were obtained for the condition involving a double solution anneal treatment (4). To determine if similar improvements could be developed in this special melt practice maraging steel, a series of small plate sections (1 x 3 x 5-in.) were cut and subjected to various heat treatments and then sectioned to provide specimens for tensile and C_v tests. The data obtained in these studies are given in Table 3 and depicted graphically in Fig. 5, as referenced to the FTID for 1-in.-thick steels. Although it appears that the double solution anneal treatments result in lower C_v values compared to the single anneal treatment, it should be noted that significantly higher YS values are developed

TABLE 3

TEST DATA FOR SOLUTION ANNEALING AND AGING TREATMENTS
ON THE SPECIAL MELT PRACTICE 18% Ni MARAGING STEEL (J-16)

| Anneal (°F) | Age (°F-hr) | 0.505-in.-diam Tensile Test Data | | | | C _v at 30°F | |
|----------------|----------------|----------------------------------|--------------|------------------|-----------|------------------------|------|
| | | 0.2% YS (ksi) | UTS (ksi) | El. in 2" (%) | RA (%) | (WR) | (RW) |
| 1650 | 850- 1 | 204.9 | 220.7 | 12.5 | 48.8 | 25 | 30 |
| 1650 | 850- 3 | 225.6 | 239.8 | 11.0 | 45.3 | 25 | 25 |
| 1650 | 850-10 | 260.5 | 266.5 | 10.0 | 44.9 | 16 | 20 |
| 1650 | 850-24 | 266.4 | 271.3 | 9.0 | 44.1 | 15 | 18 |
| 1650 | 900- 1 | 225.3 | 237.2 | 11.5 | 49.8 | 20 | 29 |
| 1650 | 900- 3 | 248.0 | 256.4 | 10.0 | 49.5 | 25 | 23 |
| 1650 | 900-10 | 267.9 | 275.3 | 10.0 | 43.6 | 17 | 19 |
| 1650 | 900-24 | 265.9 | 276.8 | 10.0 | 47.3 | 13 | 13 |
| 1650 | 950- 1 | 251.9 | 259.8 | 10.0 | 48.3 | 22 | - |
| 1650 | 950- 3 | 257.9 | 266.9 | 10.0 | 46.0 | 16 | 18 |
| 1650 | 950-10 | 249.8 | 260.2 | 10.0 | 44.3 | 17 | 18 |
| 1650 | 950-24 | 238.9 | 250.7 | 11.5 | 42.6 | 15 | 15 |
| 1650+1400 | 900- 1 | 255.5 | 259.9 | 9.0 | 47.5 | 17 | 20 |
| 1650+1400 | 900- 3 | 271.3 | 278.3 | 9.5 | 46.5 | 17 | 21 |
| 1650+1400 | 900-10 | 276.6 | 280.1 | 9.0 | 43.6 | 13 | 19 |
| 1650+1400 | 900-24 | 268.3 | 272.7 | 9.5 | 43.3 | 17 | 15 |
| 1700+1400 | 900- 1 | 250.6 | 257.1 | 8.0 | 35.5 | 21 | 23 |
| 1700+1400 | 900- 3 | 265.9 | 271.9 | 8.0 | 33.3 | 18 | 21 |
| 1700+1400 | 900-10 | 273.4 | 279.8 | 8.5 | 39.8 | 16 | 15 |
| 1700+1400 | 900-24 | 264.9 | 274.4 | 10.0 | 43.8 | 18 | 18 |
| 1800+1400 | 900- 1 | 232.9 | 245.3 | 10.0 | 40.6 | 23 | 26 |
| 1800+1400 | 900- 3 | 239.3 | 255.7 | 10.0 | 40.3 | 21 | 25 |
| 1800+1400 | 900-10 | 250.9 | 267.7 | 9.5 | 36.3 | 20 | 19 |
| 1800+1400 | 900-24 | 269.8 | 277.3 | 9.5 | 44.1 | 16 | 15 |

CHEMICAL COMPOSITION

| | | | | | | | | | |
|-----------|------------|------------|-----------|-----------|------------|------------|------------|------------|------------|
| <u>%C</u> | <u>%Mn</u> | <u>%Si</u> | <u>%P</u> | <u>%S</u> | <u>%Ni</u> | <u>%Co</u> | <u>%Mo</u> | <u>%Ti</u> | <u>%Al</u> |
| 0.007 | 0.03 | 0.04 | 0.006 | 0.005 | 18.8 | 7.58 | 4.60 | 0.48 | 0.24 |

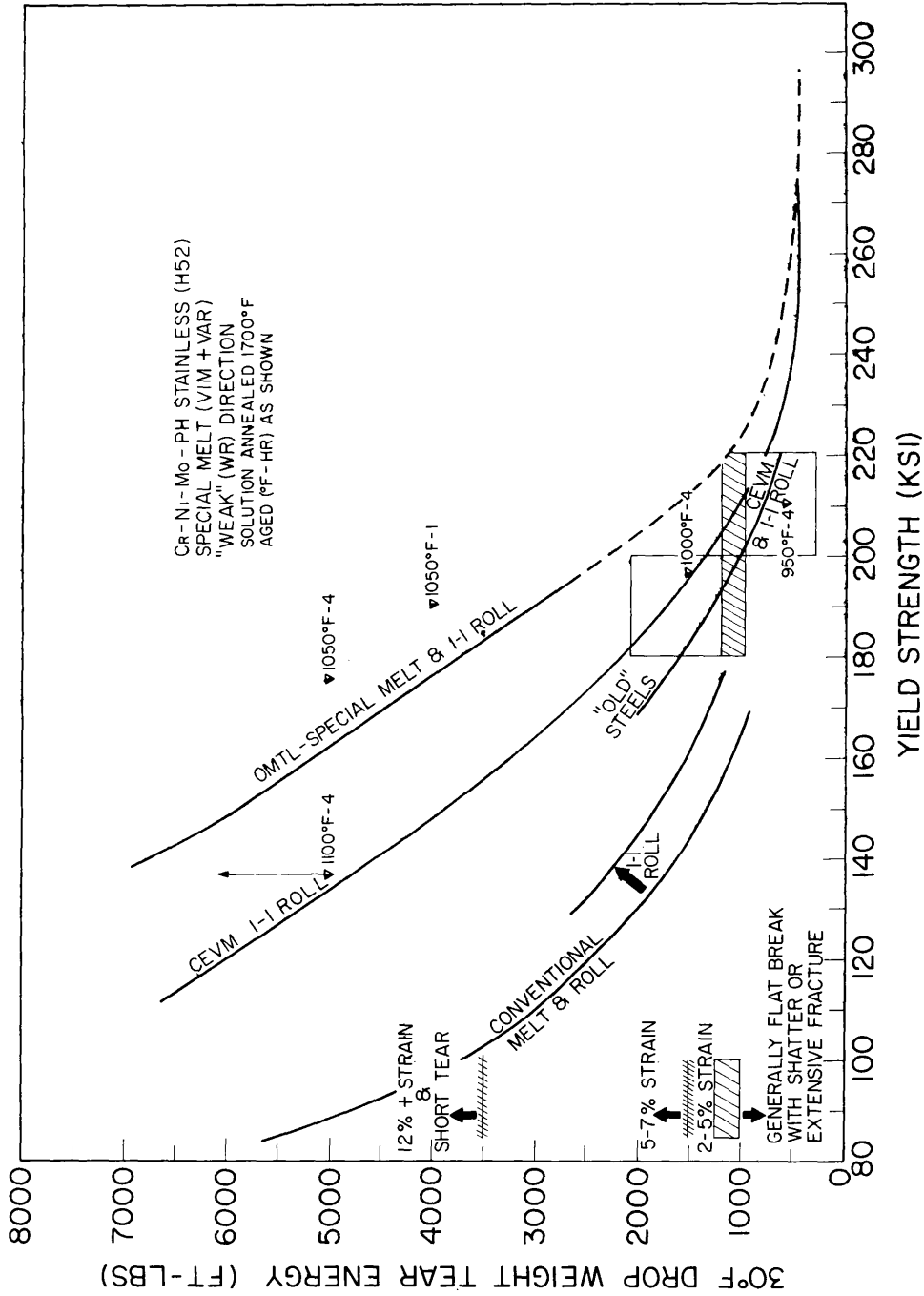


Fig.5 - Summary of Charpy V energy value YS relationships for a special melt practice 18% Ni grade 250 ksi YS maraging steel (J-16).

for any given aging time at 900°F. For all heat-treatment conditions studied, however, the C_v values were considered to be so low that DWTT studies of this steel were not considered warranted.

FRACTURE TOUGHNESS CHARACTERIZATION OF A SPECIAL MELT PRACTICE Cr-Ni-Mo PRECIPITATION HARDENING STAINLESS STEEL

Drop-weight tear test and heat-treatment studies of an experimental Cr-Ni-Mo precipitation hardening stainless steel that has recently become commercially available have been completed. This new steel is a martensitic precipitation hardening alloy that has primarily been tested as a double vacuum melted product. A highly cross-rolled, 1-in.-thick plate produced from VIM + VAR material was supplied for this investigation.

The 1-in.-thick plate (No. H52) was received in the mill-solution-annealed (1700°F) condition. Drop-weight tear test specimens were cut and hardened by aging at various temperatures and times recommended to develop maximum--and optimum--strength and toughness properties. Specimen blanks for tensile and C_v tests were cut from the fractured DWTT specimens. The chemical composition and test data developed for this steel are given in Table 4. A graphical summary of DWTT-YS and C_v -YS relationships are depicted in Figs. 6 and 7 as referenced to the FTID for 1-in.-thick steels.

Generally, the tensile and C_v values given in Table 4 were noted to be lower than those considered to be "typical" of this alloy by the producer whose results were based on tests of specimen blanks that were cut, machined, and aged after machining. In this investigation all specimens were machined in the fully hardened condition. Several of the C_v test specimens, machined from material representing the top (or bottom) one-half inch of the plate thickness, were observed to develop different amounts of shear lips on the side surfaces of the specimen. In many cases, the thickness of the shear lip on the C_v specimen surface representing centerline-thickness material was observed to be less than one-half that developed on the side of the C_v specimen representing surface material. Other indications of non-uniformity of properties throughout the thickness were observed in the fracture surfaces of DWTT specimens. Figure 8 illustrates the fracture appearance of a DWTT specimen hardened at 1000°F that developed a shear lip approximately 0.4-in.-thick on one side only.

TABLE 4

TEST DATA FOR ONE-INCH-THICK Cr-Ni-Mo
PRECIPITATION HARDENING STAINLESS STEEL (H-52)

| Aging Temp. (°F-hr) | Orien- tation* | 0.505-in. diam Tensile Test Data | | | | C _v Energy | | DWTT |
|---------------------------|-------------------|----------------------------------|--------------|-----------------|-----------|-----------------------|------|---------|
| | | 0.2% YS (ksi) | UTS (ksi) | El.in 2" (%) | RA (%) | (ft-lb) | | (ft-lb) |
| | | | | | | 30°F | 80°F | 30°F |
| 950-4 | WR | 210.8 | 222.0 | 14.0 | 56.1 | 11 | 20 | 592 |
| | RW | 207.4 | 222.3 | 15.0 | 59.8 | 14 | 20 | - |
| 1000-4 | WR | 197.6 | 202.6 | 16.5 | 66.4 | 35 | 52 | 1530 |
| | RW | 197.3 | 202.3 | 16.5 | 65.2 | 32 | 47 | 3633 |
| 1050-1 | WR | 190.7 | 197.0 | 17.0 | 64.4 | 63 | 68 | 4080 |
| | RW | 187.2 | 193.3 | 17.8 | 66.5 | 67 | 68 | 3820 |
| 1050-4 | WR | 176.1 | 182.5 | 18.5 | 69.8 | 51 | 57 | >5000 |
| | RW | 176.5 | 183.0 | 17.7 | 68.5 | 56 | 73 | >5000 |
| 1100-4 | WR | 136.9 | 161.8 | 21.0 | 70.8 | 114 | 120 | >5000 |
| | RW | 128.6 | 158.7 | 23.0 | 72.6 | 115 | 126 | >5000 |

* WR (weak)
RW (strong)

CHEMICAL COMPOSITION

| | | | | | | | | |
|-----------|------------|------------|-----------|-----------|------------|------------|------------|------------|
| <u>%C</u> | <u>%Mn</u> | <u>%Si</u> | <u>%P</u> | <u>%S</u> | <u>%Cr</u> | <u>%Ni</u> | <u>%Mo</u> | <u>%Al</u> |
| 0.044 | 0.06 | 0.02 | 0.002 | 0.004 | 12.6 | 7.88 | 2.15 | 1.14 |

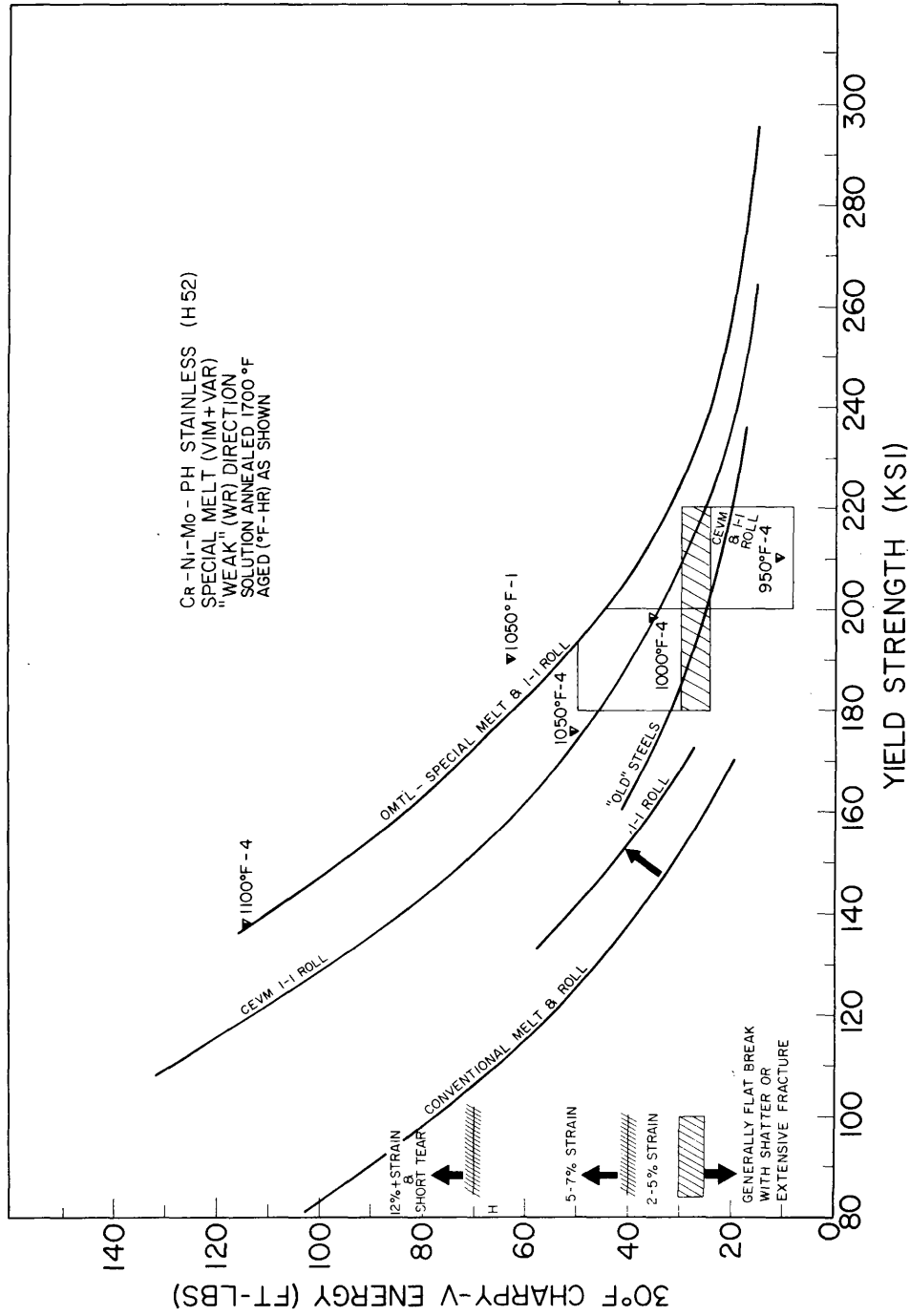


Fig. 6 - Summary of DWT-Y-S relationships for a special melt practice Cr-Ni-Mo precipitation hardening stainless steel (H-52) as referenced to the basic FTID for 1-in.-thick steels.

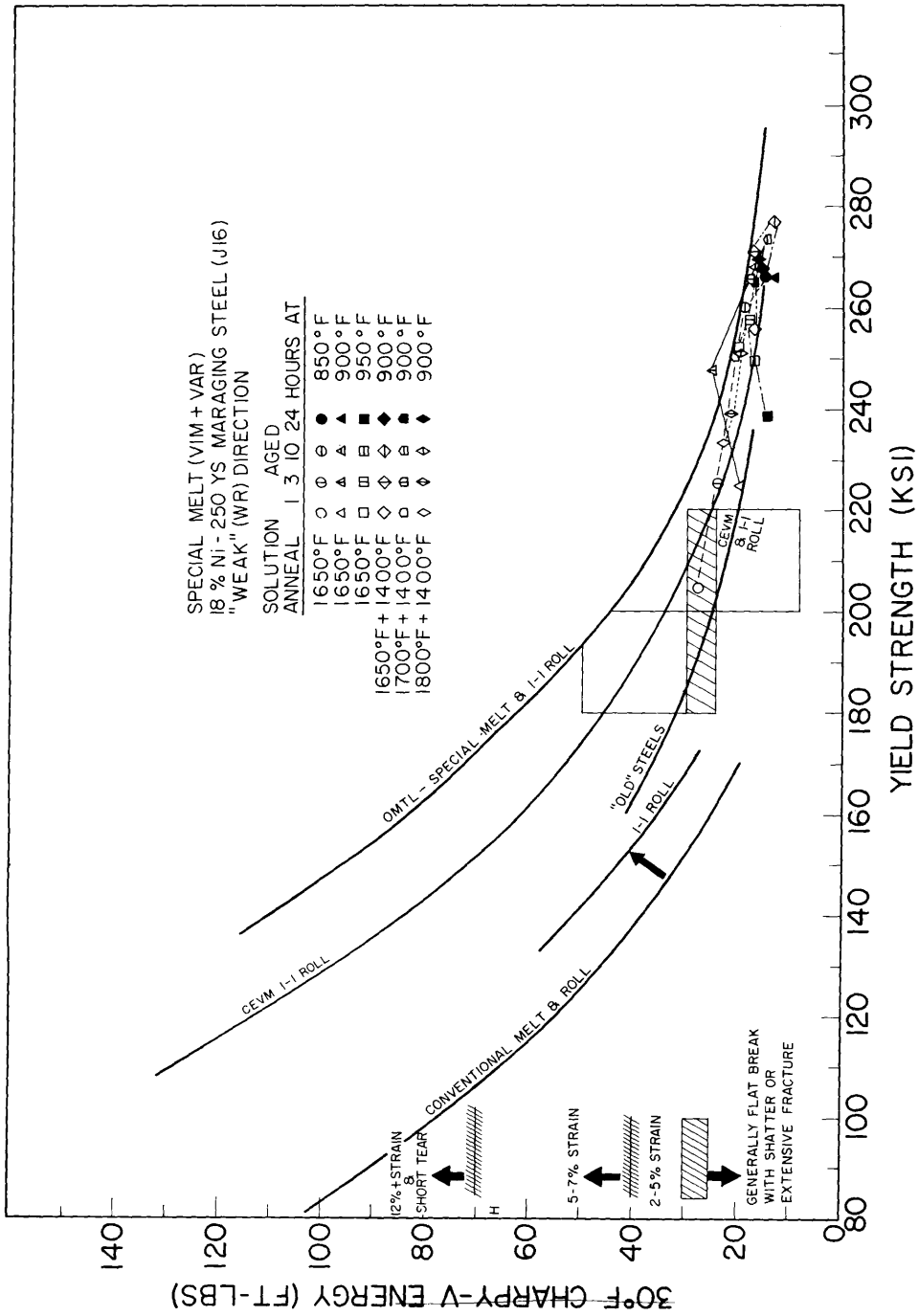


Fig. 7 - Summary of Charpy V energy value YS relationships for a special melt practice Cr-Ni-Mo precipitation hardening stainless steel (H-52).

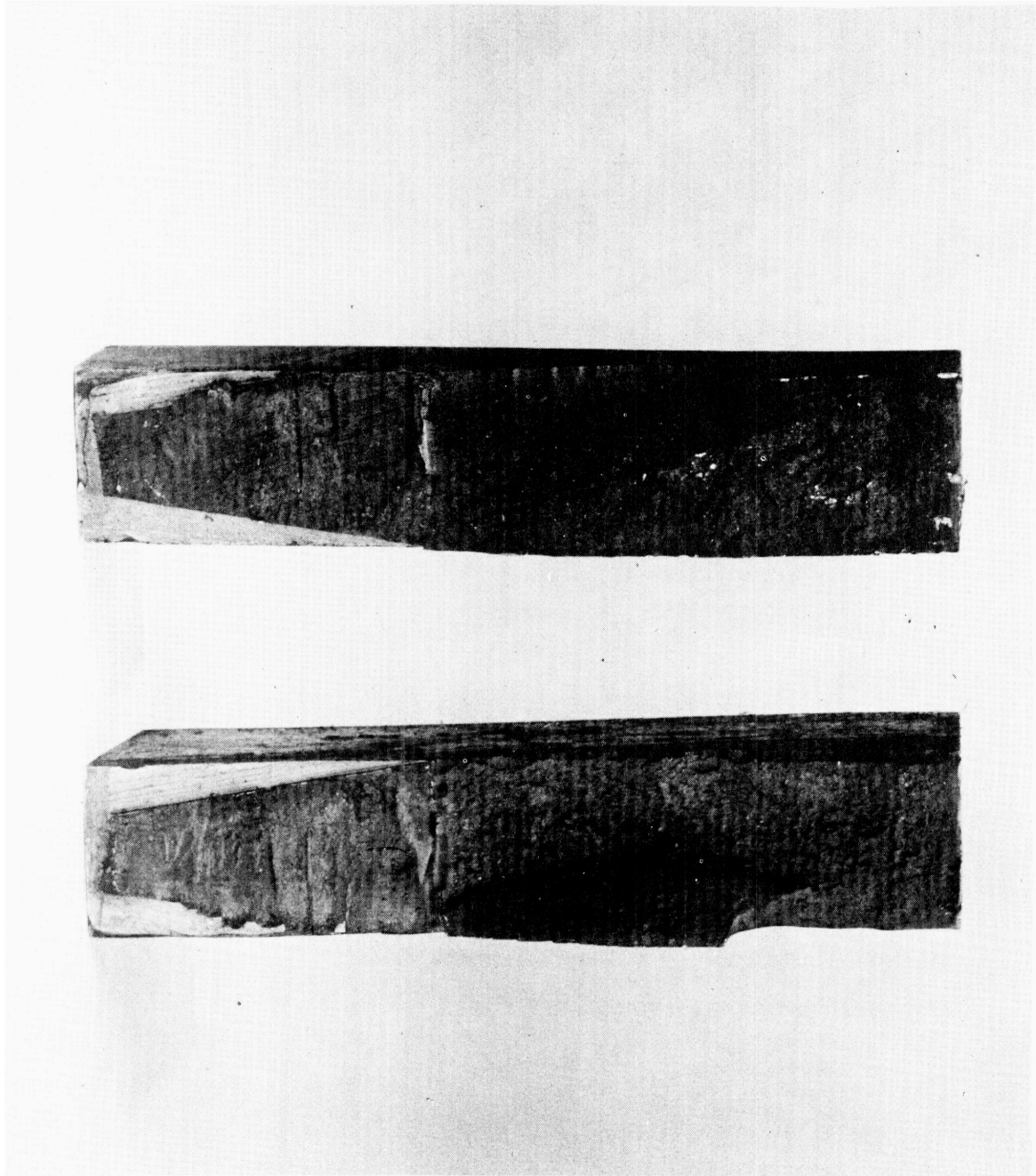


Fig. 8 - Drop-weight tear test fracture faces of a Cr-Ni-Mo precipitation hardening stainless steel alloy (H-52) illustrating significantly different amounts of shear lips developed on the two surfaces of the 1-in.-thick steel.

It is noted that in the 950°F hardened condition this steel is relatively brittle as measured by the DWTT at 30°F. Aging at 1000°F results in the development of slightly lower YS and moderately higher fracture toughness than that of the 950°F hardened condition. Optimum YS and toughness values appear to be developed by one-hour aging treatments at 1050°F, however, overaging occurs with the 4-hour treatment at this temperature as shown by the decrease in YS compared to that developed by the shorter time.

From this limited investigation, it is not possible to provide a complete evaluation of this new martensitic precipitation hardening stainless steel. A more thorough investigation of the properties of this alloy are required to determine its suitability for heavy section plate applications.

FRACTURE TOUGHNESS CHARACTERISTICS OF TITANIUM ALLOYS

(R.W. Huber and R.J. Goode)

The fracture toughness characteristics of titanium alloys have been determined for a wide variety of 1-in.-thick plate material. The drop-weight tear test (DWTT) has been demonstrated to be the most reliable test method for providing valid full thickness fracture toughness properties of 1-in. plate material. The significance of the DWTT energy values has been established by correlation with the performance of the material in the structural prototype element test--the explosion tear test (ETT). This correlation of the DWTT and ETT test results and their relationships with yield strength (YS) have been presented in the form of a Fracture Toughness Index Diagram (FTID) for 1-in.-thick plate material.

The latest FTID for titanium alloys is shown in Fig. 9 along with the DWTT data points for all materials studied. The features of the diagram and their significance are essentially the same as those described for the high strength steels in the previous section. For exact details the reader is referred to Refs. 1, 6, and 7. Briefly, below about 1500 ft-lb DWTT energy materials will propagate fractures through elastic stress regions; increasing levels of plastic strains are required for propagation of fractures for increasing values of DWTT energy above 1500 ft-lb. The

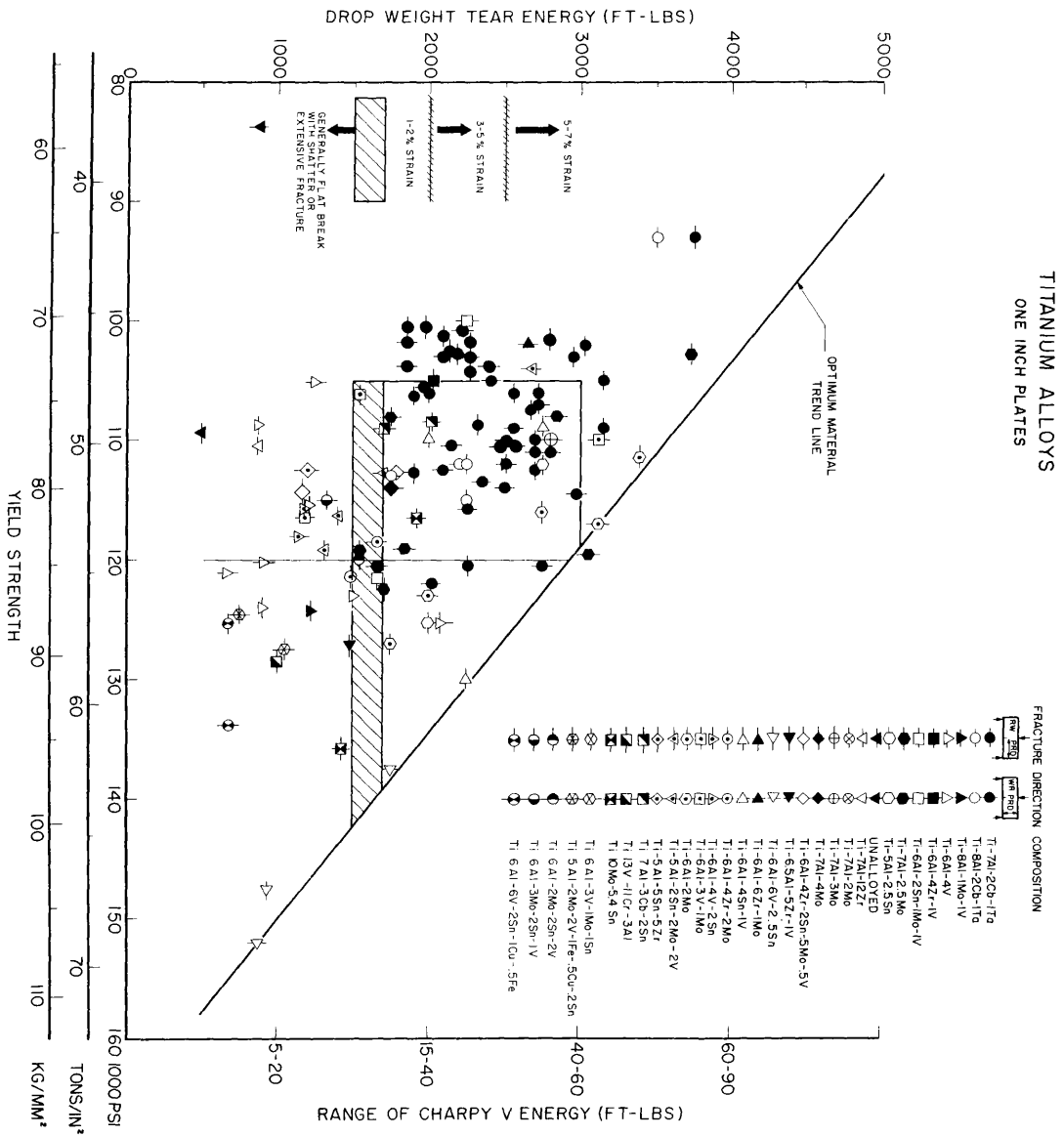


Fig. 9 - The FTID 1-in. thick titanium alloys.

impingement of the elastic-to-plastic transition band (1500-1700 ft-lb DWTT energy) with the optimum materials trend line (OMTL) indicates that for those materials having yield strengths above approximately 140 ksi YS, elastic stresses can be expected to sustain fracture propagation in all cases, and in this region fracture mechanics techniques will be required to adequately characterize fracture toughness. Between 120 and 140 ksi YS only carefully optimized alloys will be capable of developing plastic strains before crack propagation occurs. The region below 120 ksi YS is characterized by a number of alloys that require high levels of plastic strains for propagation of fractures.

RECENT FRACTURE TOUGHNESS STUDIES

Preliminary studies are underway on the second 1-in.-thick plate (Heat No. 292596) of the alloy Ti-6Al-2Cb-1Ta-0.8Mo submitted to NRL by the U.S. Navy Marine Engineering Laboratory. Drop-weight tear test energy values of 2206 ft-lb and 1966 ft-lb were measured for the RW and WR fracture directions (8) of the as-received material. These values are essentially comparable to the as-received DWTT energy values of 2384 ft-lb (RW) and 1784 ft-lb (WR) for a large 1-in.-thick plate of the same alloy composition (Heat No. 292555). A double-V type MIG weld of this alloy prepared at NRL using 1/16-in. wire of the same composition had a DWTT fracture energy of 2026 ft-lb. A similar weld vacuum-annealed at 1900°F for one hour, followed by a helium cooling, required 2560 ft-lb to fracture.

A special processing study on the Ti-6Al-2Cb-1Ta-0.8Mo alloy (Heat No. 292555) by Reactive Metals Inc. (RMI) included following the effects of processing variables upon the fracture toughness characteristics of the material. It had been demonstrated in a previous study by NRL in a cooperative study with RMI that the DWTT provided the most reliable fracture toughness information (7) for following the effects of processing. On this basis DWTT specimens representing the RW and WR fracture directions for eight different processing conditions were furnished NRL to obtain the fracture toughness information. The DWTT results are presented in Table 5. Tensile and Charpy V data are to be provided by the producer for determining the effects of the processing variables on the fracture toughness-YS relationships.

RMI PROCESSING STUDY OF Ti-6Al-2Cb-1Ta-0.8Mo ALLOY*

| Specimen No. | Frac. Dir.† | Condition | DWTT (ft-lb) |
|--------------|-------------|---------------------------------------|--------------|
| 1A L | RW | Beta annealed, air-cooled | 2618 |
| T | WR | | 1966 |
| 1B L | RW | Beta solution treated, quenched | 2266 |
| T | WR | | 2266 |
| 1C L | WR | Beta solution treated, aged | 1723 |
| T | RW | | 2146 |
| 1D L | RW | As-rolled | 2266 |
| T | WR | | 2146 |
| 2A L | RW | Alpha-beta annealed, air-cooled | 2560 |
| T | WR | | 2266 |
| 2B L | RW | Alpha-beta solution treated, quenched | 2560 |
| T | WR | | 2443 |
| 2C L | RW | Alpha-beta solution treated, aged | 2086 |
| T | WR | | 1905 |
| 2D L | WR | Alpha annealed | 2443 |
| T | RW | | 2846 |

*Heat No. 292555

†RW - Strong fracture direction

WR - Weak fracture direction

Mechanical properties for a Ti-6Al-4V (0.07 wt-% oxygen) alloy specially processed by Titanium Metals Corporation of America (TMCA) by spread rolling a 3 x 14 x 48-in. billet to a 1 x 24 x 48-in. plate at a temperature within the alpha + beta region, are shown in Table 6. The tensile data was furnished by TMCA.

TABLE 6

ALPHA + BETA SPREAD ROLLED Ti-6Al-4V ALLOY

| | | Fracture Direction† | Yield Strength (ksi) | Tensile Strength (ksi) | Drop-Weight Tear Test (ft-lb) |
|--------|---|---------------------|----------------------|------------------------|-------------------------------|
| T-100A | L | WR | 124 | 131 | 1784 |
| | T | RW | 118 | 128 | 4236 |
| T-100E | L | WR | 120 | 129 | 2846 |
| | T | RW | 116 | 127 | 3333 |

† RW - strong fracture direction; WR - weak fracture direction

These properties, if plotted on the titanium FTID, would give three points that are above the presently established OMTL. The best previous data for this alloy was plate T-6--2000 ft-lb at 125 ksi YS in the WR fracture direction and recent data on T-91, 6Al-4V (oxygen < 0.08 wt-%), showed a DWTT value of 1228 ft-lb at a 105 ksi YS level.

Several 2-in. thick titanium alloy plate specimens (27-in. long by 8-in. wide) have been studied in the DWTT. These studies were facilitated by increasing the capacity of the pendulum-type impact machine to above 10,000 ft-lb by redesigning and increasing the mass of the pendulum. The specimen brittle crack starter weld consisted of a 1 1/2-in. embrittled electron beam weld placed on the tension edge of the specimen. The DWTT data for these alloys in the mill-annealed, as-received condition are shown in Table 7.

2000 FT-LB SHOCKLESS TEAR TEST MACHINE
(E.A. Lange)

The drop-weight tear test (DWTT) was originally devised at the U.S. Naval Research Laboratory in 1962 as a

TABLE 7
DROP-WEIGHT TEAR TEST OF SOME TITANIUM ALLOYS*

| Alloy No. | Nominal Composition | Thickness (in.) | DWT (ft-lb) |
|--------------|--|--------------------|----------------|
| T 61 | Ti-7Al-2Mo | 2.06 | No Break |
| T-77 | Ti-Unalloyed 65A | 2.27 | 5780 |
| T-82 | Ti-7Al-2Cb-1Ta | 2.20 | No Break |
| T-88 | Ti-7Al-1Mo-1V | 2.03 | 8170 |
| T-89 | Ti-7Al-2Cb-1Ta | 2.61 | 9940 |
| T-90 | Ti-5Al-2Sn-2Mo-2V | 2.09 | 6680 |
| T-91 | Ti-6Al-4V (0.08 wt-% max. O ₂) | 2.14 | 9320 |
| T-92 | Ti-6Al-6V-2Sn-1Cu-0.5Fe | 2.10 | 3190 |
| T-93 | Ti-6Al-3V-1Mo | 2.10 | 8260 |
| T-94 | Ti-7Al-2.5Mo | 2.26 | 9760 |
| T-95 | Ti-6Al-4V (0.12 wt-% O ₂) | 2.19 | 4070 |
| T-96 | Ti-6Al-2Cb-1Ta-0.8Mo | 2.55 | No Break |
| T-98 | Ti-3.5Al | 1.91 | No Break |

* Mill annealed specimens (2x8x27") with 1-1/2" crack starter weld.

practical means for determining the fracture toughness of full thickness sections of high strength metals. Extensive testing has been conducted with a 5000 ft-lb single pendulum machine for a broad program including high strength steels, titanium alloys, and aluminum alloys. A 5000 ft-lb capacity machine was found adequate for assessing the fracture toughness of 1-in.-thick plate of all of these materials, and the full spectrum picture of the fracture characteristics of high strength metals in 1-in.-thick plate is kept current as one aspect of the Advanced High Strength Structural Materials Program of the Metallurgy Division.

The DWTT was also recommended as a sensitive test for establishing the critical temperature for the fracture transition behavior of structural steel in sections thinner than 5/8-in., which is the minimum thickness limit for establishing the critical temperature--NDT (nil-ductility-transition)--using ASTM E208 test methods. The DWTT and fracture appearance criterion has been extensively studied and found to be a useful parameter for predicting the performance of line pipe steel (9). Meanwhile, at NRL a small specimen which could be used for crack initiation as well as crack propagation studies has been under development. Optimization studies have evolved a specimen having the dimensions of 5/8 x 1 5/8 x 7-in., which has proven to indicate more correctly the fracture transition with temperature of heavy section steel than the conventional engineering test, Charpy V (1). When the potential of the subsized specimen for providing dynamic K_{IC} , fracture appearance, and tear energy data was apparent, a test machine with a capacity scaled to the small specimen was procured. The new machine was not a simple scale model of the 5000 ft-lb machine because in addition to the requirement for accurate measurement of tear energy, a requirement for shockless operation was specified so that the machine could be used in hot cells which are steel lined and contain glass windows and sensitive instruments. A double pendulum design of 2000 ft-lb capacity was specified and detail design and construction was contracted to Southwest Research Institute. The machine is currently being instrumented at NRL for digital readout of energy and an electrical signal for load on the tup of the hammer. Pertinent design features of the machine are shown in Fig. 10.

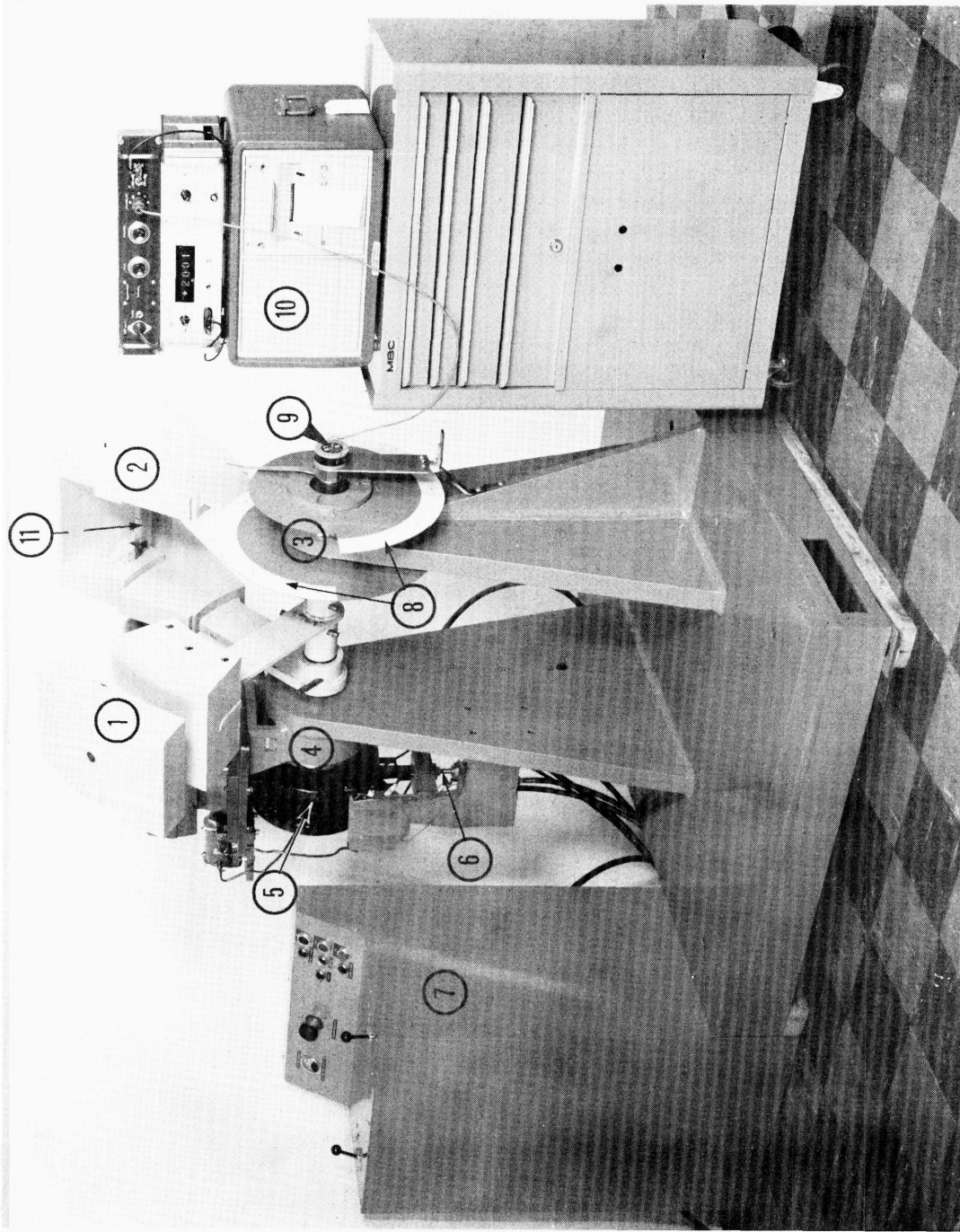


Fig. 10 - 2000 ft-lb Shockless Tear Test Machine: (1) Hammer [332 lb], (2) Anvil [337 lb], (3) One-way clutch for hammer [clockwise], (4) One-way clutch for anvil [counter-clockwise], (5) Cocking drive mechanism, (6) Trigger, (7) Control console, (8) Energy dials, (9) Sine-cosine rotary potentiometer, (10) Digital readout equipment, (11) Specimen [5/8 x 1-5/8 x 7-in.].

As previously stated, the double pendulum design was incorporated to eliminate errors in energy measurement due to movement of the machine relative to the floor and to minimize the shock transmitted to the floor during test. The machine is compact in design; the weights of the hammer and the anvil are 332 and 337 lb, respectively, and when they are released from a 145° cocked position (Fig. 10), the drop height is 3 ft which provides a constant initial potential energy of 2000 ft-lb. The specimen is held on the anvil with spring clips, and the center of percussion of the anvil with test specimen in place is within 0.5% of the center of percussion of the hammer. This feature permits the machine to be installed with no special floor mounting or without mechanical fastening. The one-way feature for the rotation of the hammer and the anvil is accomplished with clutches; this permits the terminal energy of the pendulums to be a static reading on either the dials or electrical instrumentation. The clutches and bearings introduce a full-swing fractional error of 7 ft-lb, but this error is constant and is accounted for in the calibration of the dials and the electrical readout. The accuracy of the energy value is within 0.5% of reading or 2 ft-lb whichever is greater. Precise readout can be obtained either from the dials which are divided into 10 ft-lb increments or the digital instrument which indicates in four figures or 1 ft-lb increments.

A special tup is currently being developed which will enable force-time data to be taken during an impact test. The special tup is instrumented with strain gages and the load signal will be recorded with either an oscilloscope or a tape recorder. When this instrumentation is completed, dynamic fracture toughness values can be determined in terms of fracture mechanics K_{Ic} parameters and will be appearing in later issues of this Quarterly series.

PLANE STRAIN FRACTURE TOUGHNESS TESTING OF TITANIUM AND ALUMINUM ALLOYS

(C.N. Freed and R.J. Goode)

The resistance of a material to fracture can be evaluated by measuring the energy required to initiate the extension of a crack in the material and that energy

needed to cause the crack to propagate. No single test has been devised which can separately measure both events; rather, initiation and propagation must be evaluated individually.

The energy required to initiate extension of a crack from a simulated flaw may be determined by fracture mechanics. In particular, plane strain fracture toughness, K_{Ic} , will describe initial crack extension when the flaw is surrounded by an essentially elastic stress field. The K_{Ic} energy value is believed to be a material invariant, and is dependent only upon temperature and strain rate.

The resistance of a material to crack propagation is measured by the drop-weight tear test (DWTT). In this test, a moving crack is impinged upon the research material, and the energy required to fracture the specimen is recorded. A correlation has been made between the DWTT and the explosion tear test (ETT) performance, a structural prototype test (1). This correlation is pertinent for the toughness region in which small plastic strain overloads are needed for propagation of the fracture in the ETT. In the ETT as normally conducted, when a crack propagates under elastic conditions, a correlation between these tests is not possible.

Since the plane strain fracture toughness measurement K_{Ic} implies the use of linear elastic fracture mechanics, it is only in the region in which a crack will extend under elastic stresses that K_{Ic} may be measured. One objective of the Strength of Metals Branch is to determine whether a correlation exists between the DWTT and K_{Ic} in the elastic stress region.

EXPERIMENTAL DETAILS AND MATERIALS

The mechanical properties of four aluminum and two titanium alloys are presented in Table 8. The aluminum alloys were tested in the as-received condition while the titanium alloys were heat treated as noted.

The K_{Ic} data in this report was obtained with two types of specimens: the single-edge-notch (SEN) and the notch-bend (NB). The dimensions used for the SEN specimens were 5x13x1-in. and 4 1/2x12x1-in.

TABLE 8
MECHANICAL PROPERTIES OF SEVERAL ALUMINUM AND TITANIUM ALLOYS

| Nominal Com- position and Code No. | Frac. Dir. | YS (ksi) | UTS (ksi) | Elong. (%) | RA (%) | DWT at 32°F (ft-lb) | Cv at -80°F (ft-lb) | Cv at 32°F (ft-lb) | Heat Treatment |
|--|---------------|-------------|--------------|---------------|-----------|------------------------------|---------------------------|--------------------------|---------------------------------------|
| 2020 (A-6) | WR | --1 | --1 | --1 | --1 | 107 | --1 | --1 | As received |
| 2219-T851(A-15) | RW | 59.3 | 73.4 | 10 | 22.7 | 514 | -- | 5 | As received |
| 7079-T6(A-13) | WR | 74.9 | 85.4 | -- | -- | 111 | -- | 2 | As received |
| 7106-T63(A-17) | WR | 52.5 | 60.8 | 13.9 | 40.0 | 573 | -- | 8 | As received |
| Ti-6Al-4Zr-2Mo (T-55B) | WR | 140.2 | 153.7 | 7.0 | 11.7 | 748 | 17 | 17 | 1800°F/1 hr/WQ then 1000°F/2 hr/AC |
| Ti-6Al-4V-2Sn (T-67A) | RW | 129.8 | 141.2 | 8.0 | 12.9 | 540 | 22 | 24 | 1775°F/1 hr/WQ then 1000°F/2 hr/AC |
| Ti-6Al-4V-2Sn (T-67B) | RW | --1 | --1 | --1 | --1 | --1 | --1 | --1 | 1675°F/1 hr/WQ no aging treatment |

¹Data is being obtained.

(width x length x thickness). The ratio of the distance between loading pin centers to the width was similar to that employed by A.S. Sullivan and the experimental compliance calibration of Ref. 10 was used in the calculation of K_{Ic} . The notched-bend specimen was recommended by J. Srawley and W. Brown (11). The dimensions were 2.5x20x1-in. (width x length x thickness), and the tests were conducted in a four-point-loading jig. The onset of crack growth was detected with a displacement gage inserted in the edge notch.

Side grooves were machined in several of the alloys to accentuate the deflection at crack instability. The grooves contained an included angle of 60° and had a notch-root radius of 0.002-in. The symmetrical grooves, which were machined across the width of the specimen parallel to the edge-notch, are described by the ratio of the thickness between apexes of the grooves, B_N , to the thickness prior to grooving, B . The calculation to determine K_{Ic} for the side-grooved specimen is presented in (6).

K_{Ic} DATA FOR FOUR ALUMINUM ALLOYS

Plane strain toughness values have been determined for four aluminum alloys: 2020, 2219-T851, 7079-T6, and 7106-T63. The experimental data for these alloys is compiled in Table 9. Each specimen was fatigued to produce a crack approximately 0.10-in. at the tip of each edge notch; the fatigue pressure was limited to less than one-half the yield strength (YS) in most cases. The plastic zone correction factor was insignificant and was not used to establish K_{Ic} .

For the two alloys 2020 and 7079-T6, sufficient material was available to test only one specimen each. The calculated K_{Ic} values of 16,000 and 22,000 $\text{psi}\sqrt{\text{in.}}$ for 2020 and 7079-T6, respectively, were the lowest which have been found in this program.

The alloy 2219-T851 was tested in the RW fracture direction with both smooth (no side grooves) and side-grooved specimens. The K_{Ic} indication of 37,000 $\text{psi}\sqrt{\text{in.}}$ for the smooth specimens is similar to 35,000 $\text{psi}\sqrt{\text{in.}}$ value calculated for the side-grooved tests. (The load used to calculate K_{Ic} for the smooth specimens was the

TABLE 9
PLANE STRAIN FRACTURE TOUGHNESS DATA FOR SEVERAL ALUMINUM ALLOYS

| Alloy | Frac. Dir. | Thick-ness Between Side grooves B _n (in.) | Total thick-ness B (in.) | $\frac{B_n}{B} \times 100\%$ (%) | Width W (in.) | Crack Length a _c (in.) | $\frac{a_c}{W}$ | Load at K _{Ic} P (lbs.) | K _{Ic} (psi√in.) | Nom-inal Stress to Yield Stress $\frac{\sigma_n}{\sigma_{ys}}$ | Per-cent Shear | Plas-tic Zone Size ^a r _y (in.) |
|-----------|------------|--|--------------------------|----------------------------------|---------------|-----------------------------------|-----------------|----------------------------------|---------------------------|--|----------------|--|
| 2020 | WR | No side grooves | 1.36 | -- | 5.73 | 1.92 | 0.34 | 28000 | 16000 | -- | 0 | -- |
| 2219-T851 | RW | No side grooves | 0.97 | -- | 4.50 | 1.51 | 0.34 | 39000 | 37000 | 0.58 | 76 | 0.06 |
| 2219-T851 | RW | 0.90 grooves | 0.97 | 93 | 4.50 | 1.49 | 0.33 | 36300 | 35000 | 0.56 | -- | 0.05 |
| 2219-T851 | RW | 0.90 grooves | 0.97 | 93 | 4.50 | 1.47 | 0.33 | 37200 | 35000 | 0.57 | -- | 0.05 |
| 7079-T6 | WR | No side grooves | 1.02 | -- | 4.50 | 1.53 | 0.34 | 23800 | 22000 | 0.27 | 0 | 0.01 |
| 7106-T63 | WR | No side grooves | 0.97 | -- | 4.50 | 1.67 | 0.33 | (48000) [□] | (43000) [□] | 0.76 | 73 | 0.11 |
| 7106-T63 | WR | No side grooves | 0.97 | -- | 4.50 | 1.66 | 0.33 | (46000) [□] | (40000) [□] | 0.70 | 84 | 0.09 |
| 7106-T63 | WR | 0.88 grooves | 0.97 | 91 | 5.00 | 1.60 | 0.32 | 45400 | 40000 | 0.70 | -- | 0.09 |
| 7106-T63 | WR | 0.87 grooves | 0.97 | 90 | 5.00 | 1.58 | 0.32 | 47400 | 42000 | 0.73 | -- | 0.10 |
| 7106-T63 | WR | 0.87 grooves | 0.97 | 90 | 5.00 | 1.84 | 0.37 | 38000 | 41000 | 0.73 | -- | 0.10 |

[□] Load at which crack initiated was difficult to determine and could only be estimated.

$$r_y = \left(\frac{K_{Ic}}{\sigma_{ys}} \right)^2 \frac{1}{2\pi}$$

point of abrupt departure from linearity of the load-deflection curve; maximum load was used for the side-grooved specimens as the curve was virtually linear below that load.)

It was not possible to determine K_{Ic} with certainty for 7106-T63 unless side grooves were employed. The smooth specimens evidenced a deviation from linearity so gradual that the load at which crack extension commenced could only be estimated. However, when the specimens were side grooved to a depth of 5% of the thickness on each side ($B_N/B = 0.9$), the straight-line portion of the curve extended to maximum load. The plane strain toughness values ranged between 40,000 to 42,000 $\text{psi}\sqrt{\text{in.}}$ for the grooved specimens.

For the aluminum alloys reported herein, the calculated plastic zone was well contained within the thickness of the specimen, and the nominal stress was below the yield stress (Table 9). While fatiguing the 7106-T63 specimens, it was necessary to exert a pressure greater than one-half the yield stress. This alloy will be re-tested to determine whether the fatigue pressure affected the K_{Ic} value.

K_{Ic} DATA FOR TWO TITANIUM ALLOYS

The specimens of the titanium alloy Ti-6Al-4Zr-2Mo (T-55) were separately solution annealed at 1800°F for one hour and water-quenched, then aged at 1000°F for two hours and air cooled. The K_{Ic} data was ascertained for the WR fracture direction using both smooth and side-grooved specimens (Table 10). Of the eight specimens tested, six indicate that K_{Ic} should lie between 92,000 and 102,000 $\text{psi}\sqrt{\text{in.}}$. Two SEN specimens indicated lower K_{Ic} numbers (74,000 and 77,000 $\text{psi}\sqrt{\text{in.}}$), but the macrofracture surface contained no shear lips which may indicate that the β -transus temperature of $1840 \pm 15^\circ\text{F}$ had been exceeded. (The NB specimens also evidenced little macro-shear but as the loading arrangement was entirely different from the SEN specimens, no comparison should be made between them.)

Specimens of a second alloy, Ti-6Al-4V-2Sn (T-67), was given two different heat treatments and tested in the RW fracture direction. Heat treatment A

TABLE 10
 PLANE STRAIN FRACTURE TOUGHNESS DATA FOR TITANIUM ALLOYS:
 Ti-6Al-4Zr-2Mo (T-55) AND Ti-6Al-4V-2Sn (T-67)

| Alloy | Frac. Dir. | Thick-ness Between Side Grooves B _n (in.) | Total Thick-ness B (in.) | $\frac{B_n}{B}$ X100% (%) | Width W (in.) | Crack Length a _c (in.) | $\frac{a_c}{W}$ | Load at K _{Ic} P (lbs.) | K _{Ic} (psi $\sqrt{in.}$) | Nom-inal Stress to Yield Stress $\frac{\sigma_N}{\sigma_{YS}}$ | Per-cent Shear | Plas-tic Zone Size [Ⓔ] r _y (in.) |
|--------------------|------------|--|--------------------------|---------------------------|---------------|-----------------------------------|-----------------|----------------------------------|-------------------------------------|--|----------------|--|
| T-55B | WR | 0.97 | 1.09 | 89 | 5.01 | 1.57 | 0.31 | 119000 | 92000 | 0.62 | -- | 0.07 |
| T-55B | WR | 0.97 | 1.09 | 89 | 5.00 | 1.60 | 0.32 | 119700 | 95000 | 0.62 | -- | 0.07 |
| T-55B | WR | no side grooves | 1.08 | -- | 5.00 | 1.64 | 0.33 | 99000 | 77000 | 0.46 | 0 | 0.05 |
| T-55B | WR | no side grooves | 1.08 | -- | 5.00 | 1.65 | 0.33 | 94300 | 74000 | 0.45 | 0 | 0.04 |
| T-55B | WR | no side grooves | 1.09 | -- | 5.01 | 1.60 | 0.32 | 134400 | 102000 | 0.63 | 39 | 0.08 |
| T-55B | WR | no side grooves | 1.08 | -- | 5.00 | 1.71 | 0.34 | 119000 | 97000 | 0.61 | 32 | 0.08 |
| T-55B [Ⓙ] | WR | no side grooves | 1.07 | -- | 2.50 | 0.83 | 0.33 | 13900 | 92000 | 0.85 | 8 | 0.07 |
| T-55B [Ⓚ] | WR | no side grooves | 1.07 | -- | 2.50 | 0.69 | 0.28 | 17100 | 98000 | 0.79 | 8 | 0.08 |
| T-67A | RW | no side grooves | 0.96 | -- | 5.00 | 1.68 | 0.34 | 98700 | 88000 | 0.61 | 28 | 0.07 |
| T-67A | RW | no side grooves | 0.93 | -- | 5.00 | 1.62 | 0.32 | 87200 | 78000 | 0.51 | 37 | 0.06 |
| T-67A | RW | no side grooves | 1.00 | -- | 5.00 | 1.63 | 0.33 | 85500 | 71000 | 0.48 | 7 | 0.05 |
| T-67A | RW | 0.84 | 0.93 | 90 | 5.01 | 1.59 | 0.32 | 100300 | 90000 | 0.64 | -- | 0.08 |
| T-67A [Ⓛ] | RW | no side grooves | 0.77 | -- | 2.50 | 0.62 | 0.25 | 10800 | 79000 | 0.68 | 0 | 0.06 |
| T-67B | RW | no side grooves | 0.99 | -- | 5.00 | 1.93 | 0.39 | 89600 | 96000 | -- [Ⓜ] | 13 | -- [Ⓝ] |
| T-67B | RW | no side grooves | 1.00 | -- | 5.01 | 1.83 | 0.37 | 107300 | 105000 | -- | 12 | -- |
| T-67B | RW | 0.95 | 1.02 | 93 | 5.01 | 1.56 | 0.31 | 132400 | 106000 | -- | -- | -- |
| T-67B | RW | 0.94 | 1.02 | 92 | 5.00 | 2.23 | 0.45 | (69000) [Ⓟ] | (95000) [Ⓠ] | -- | -- | -- |
| T-67B [Ⓡ] | RW | no side grooves | 0.78 | -- | 2.51 | 0.94 | 0.38 | 11100 | 112000 | -- | 0 | -- |

[Ⓙ] Notch bend specimen tested by four-point loading.

[Ⓚ] Load at which crack initiated was difficult to determine and could only be estimated.

[Ⓛ] Yield strength has not yet been determined.

$$\textcircled{z} r_y = \left(\frac{K_{Ic}}{\sigma_{YS}} \right)^2 \frac{1}{2\pi}$$

Heat Treatments:

T-55B - 1800°F/1 hr/WQ solution anneal followed by 1000°F/2 hr/AC age.
 T-67A - 1775°F/1 hr/WQ solution anneal followed by 1000°F/2 hr/AC age.
 T-67B - 1675°F/1 hr/WQ solution anneal. No aging heat treatment.

involved a solution anneal at 1775°F for one hour and water quenched, followed by an aging treatment at 1000°F for two hours and air cooled. The solution anneal was below the β -transus temperature of 1815 \pm 15°F. The K_{IC} number for this heat treatment averaged 81,000 psi/ $\sqrt{\text{in}}$. for SEN and NB specimens.

Five additional specimens were given a solution anneal of 1675°F for one hour and water quenched (heat treatment B). These specimens, which were not aged, indicated an average K_{IC} of 105,000 psi/ $\sqrt{\text{in}}$.

CORRELATION OF β_{IC} WITH DWTT AND YIELD STRESS WITH K_{IC}

In the Tenth Quarterly Report (4) a preliminary correlation was presented between K_{IC} and DWTT energy for titanium alloys. The recent completion of mechanical tests has permitted β_{IC} ($[K_{IC}/\sigma_{ys}]^2 l/B$) to be plotted against DWTT energy (Fig. 11). It is more meaningful to correlate β_{IC} with DWTT energy as $(K_{IC}/\sigma_{ys})^2$ is a characteristic dimension of the plastic zone, and it is this plasticity that resists the propagation of a crack in the DWTT. Furthermore, since $(K_{IC}/\sigma_{ys})^2$ is proportional to the plastic zone size, dividing this by the thickness, B, provides an indication of the elastic constraint controlled by the stress state surrounding the plastic zone.

It is necessary to consider several factors when studying the correlation presented in Fig. 11. First, the K_{IC} test is conducted at a very slow strain rate while the DWTT is a high strain rate impact test. If the material is strain-rate sensitive, the plastic zone (r_y) at the tip of the crack will not be the same size in both tests. (Since r_y varies inversely with $[YS]^2$, if YS is strain rate dependent, then r_y will change significantly with strain rate.) Fortunately, titanium alloys do not appear to be particularly strain-rate sensitive within the range of strain rates involved in these tests.

A second point to be considered is that the initiation of a crack in the brittle weld of the DWTT specimen requires energy which does not directly contribute to the formation of the plastic zone. The energy necessary to fracture the brittle weld is estimated to be between 150 and 200 ft-lb. This is indicated in Fig. 11 by the fact that the band of points does not originate at zero DWTT energy, but is offset on the DWTT energy axis by an amount approximating the energy absorbed by the brittle weld.

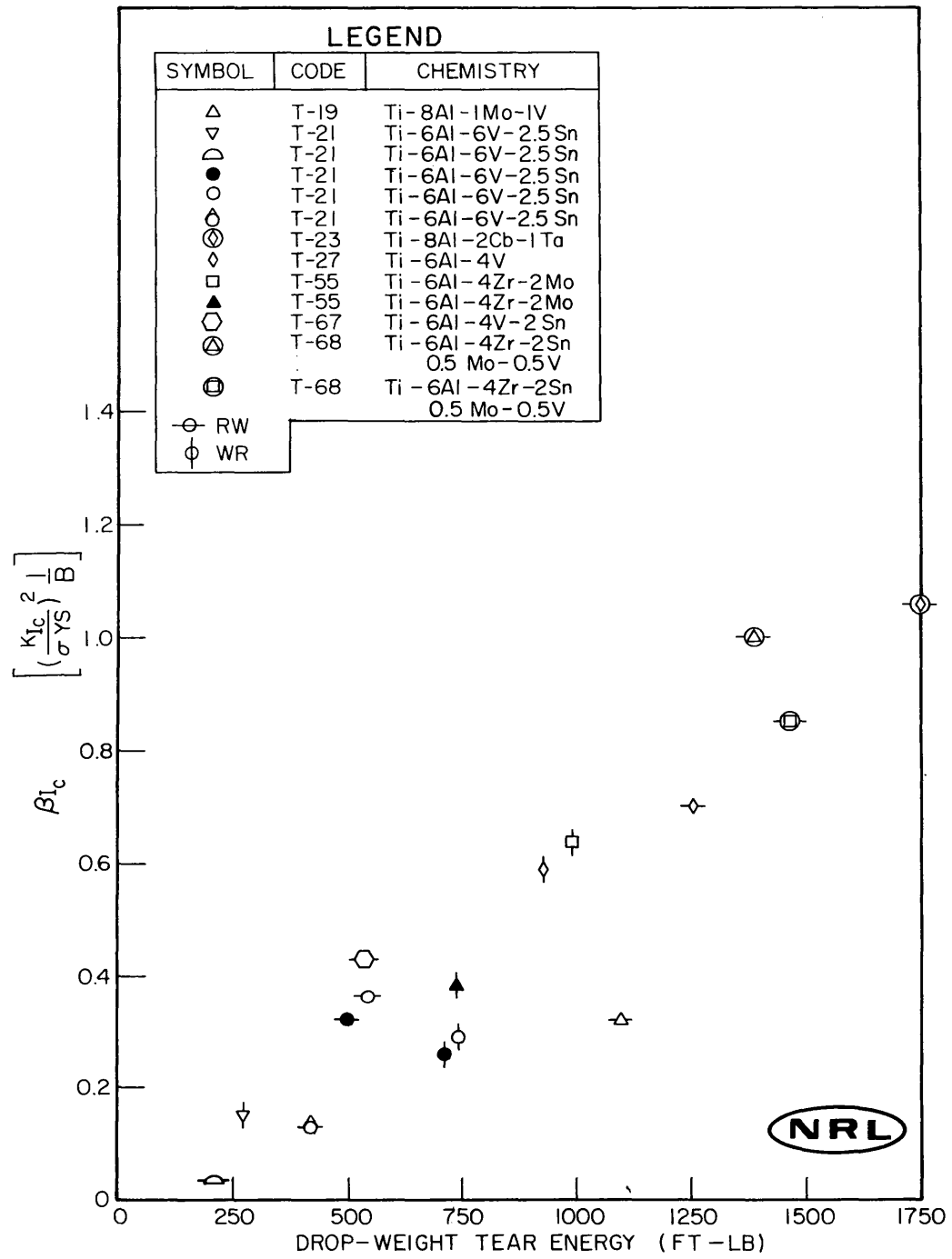


Fig. 11 - Preliminary correlation of βI_c versus drop-weight tear energy for several titanium alloys

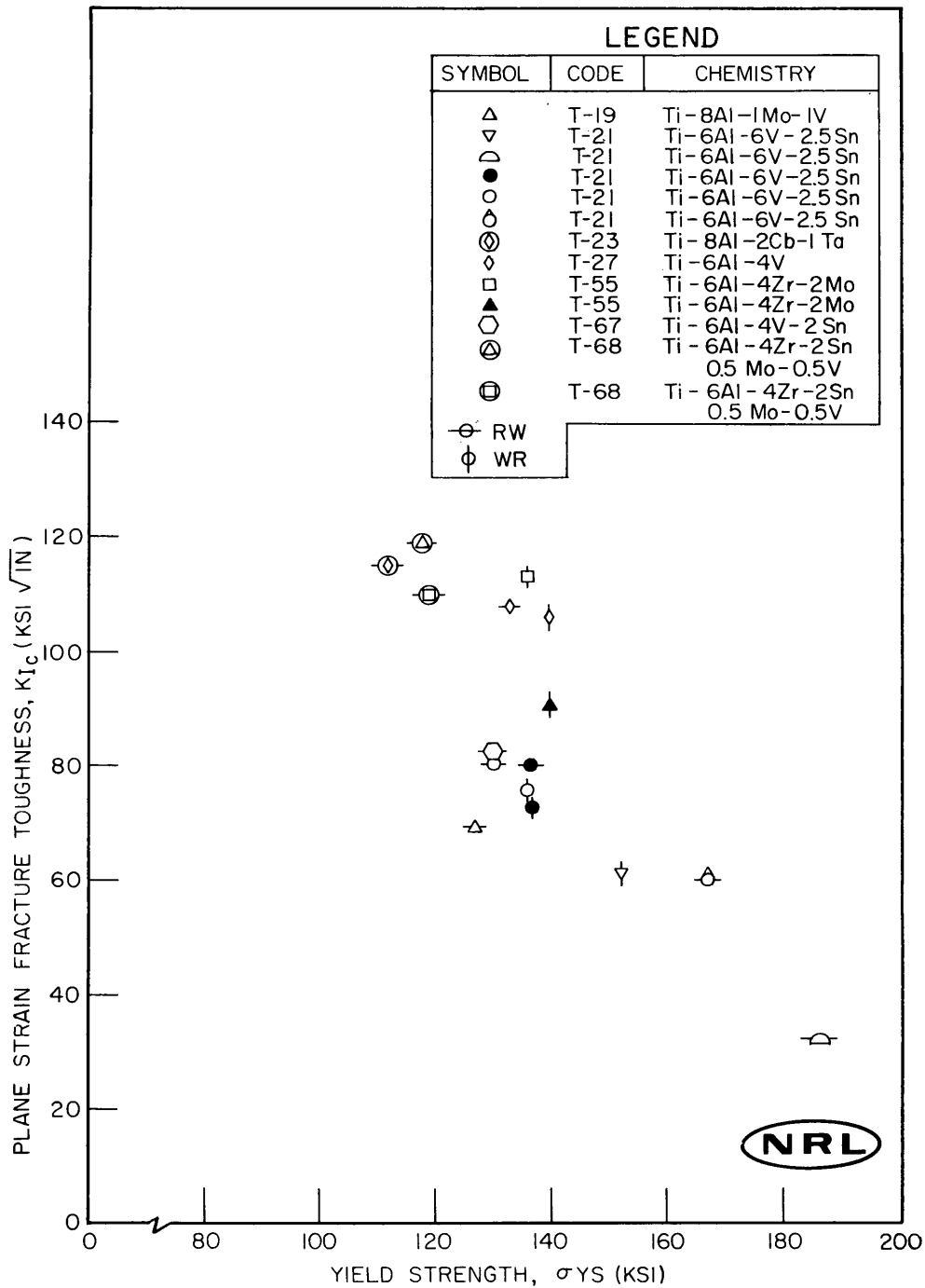


Fig. 12 - Correlation of Plane strain fracture toughness, K_{Ic} , with yield strength for several titanium alloys.

The last factor to be considered between the two tests is the fundamental difference in the state of stresses around the plastic zone. Plane strain fracture toughness requires that the plastic zone be surrounded by an elastic stress field which provides constraint sufficient to prevent relaxation from the surface. This condition exists in only the most brittle DWTT specimens. In most of the drop-weight tear tests on titanium, shear lips are formed which occupy a significant portion of the fracture surface. This indicates that the plastic zone was not sufficiently constrained to provide plane strain conditions; rather, the test was conducted under mixed-mode or plane stress conditions.

In spite of these factors which will affect a correlation between K_{IC} and the DWTT, preliminary results for several titanium alloys indicate that a relationship between the two tests does exist. A scatter band would be expected because of the factors previously cited and additional test variables including individual specimen heat treatment. Further tests are being conducted to better define the trend of the points in Fig. 11.

In Fig. 12, the YS values (at 0.2% offset) of the titanium alloys shown in Fig. 11 are plotted against plane strain fracture toughness. An inverse relationship is evident indicating that as the yield stress increases, K_{IC} will decrease. The YS values range from a low of 112 ksi to a high of 186 ksi for the alloy Ti-6Al-6V-2.5Sn.

LOW CYCLE FATIGUE CRACK PROPAGATION IN
9Ni-4Co-0.25C STEEL IN AIR AND 3.5 PERCENT SALT WATER
(T.W. Crooker and E.A. Lange)

Current interest in materials for high performance structures has focused attention on new alloy systems possessing improved potentials for high strength-to-density ratios, high fracture toughness, and immunity from environmental attack. Successful service applications involving new high strength materials in structures requiring welded joints can be dependent upon resistance to failure from the propagation of low cycle fatigue cracks. Such cracks are readily initiated

from cracklike weld defects, which escape detection in complex structures because of practical deficiencies in manufacturing and nondestructive testing techniques. This problem is further heightened by the fact that strain intensifications are likely to occur in structures around points of geometric discontinuity, such as welded joints. Also, it is not uncommon for structures to operate in an aggressive environment, such as sea water, which can be expected to accelerate flaw growth.

Therefore, investigations are underway to define and evaluate the factors which control the growth of low cycle fatigue cracks and to assess their effects on various materials. Such knowledge is essential in selecting optimum materials and predicting the reliable service life of cyclically-loaded structures.

The low cycle fatigue crack propagation characteristics of a spectrum of materials, both low strength and high strength, ferrous and nonferrous, have been discussed in previous reports (2-4, 6, 12-18). This is a progress report on 9Ni-4Co-0.25C steel at a yield strength (YS) level of 180 ksi. The testing procedures employed are the same as those described in the references so as to provide a common basis for comparisons with the results of previous studies.

TEST MATERIAL

Low cycle fatigue crack propagation tests were conducted on two samples of 9Ni-4Co-0.25C steel. Both samples were obtained from the same heat and were given the same heat treatment, but were rolled to one-inch plate by different procedures. The material designated J14 is straight-rolled, and the material designated J15 is 1:1 cross-rolled.

These materials were tested in the as-received mill heat-treated condition. Chemical compositions and mechanical properties of these materials are given in Tables 11 and 12, respectively. In addition, drop-weight tear test (DWTT) results on these materials are reported in Ref. 2.

TABLE 11
 CHEMICAL COMPOSITION OF 9Ni-4Co-.25C STEELS*

| NRL Code | Element (Weight - Percent) | | | | | | | | | | |
|----------|----------------------------|-----|-----|------|------|------|-----|-----|------|-----|--|
| | C | Mn | Si | P | S | Ni | Cr | Mo | Co | V | |
| J14 | .25 | .29 | .01 | .004 | .008 | 8.62 | .40 | .48 | 3.76 | .11 | |
| J15 | .25 | .28 | .01 | .006 | .008 | 8.31 | .40 | .48 | 3.78 | .11 | |

*NRL Data

TABLE 12
 MECHANICAL PROPERTIES OF 9Ni-4Co-.25C STEELS*

| NRL Code | Fracture Orientation** | 0.2% YS (ksi) | UTS (ksi) | ELONG (%) | RA (%) | C _v @ 30°F (ft-lb) | DWTT @ 30°F (ft-lb) |
|----------|------------------------|---------------|-----------|-----------|--------|-------------------------------|---------------------|
| J14 | WR | 180.3 | 196.4 | 15.0 | 48.0 | 31 | 1173 |
| J14 | RW | 180.0 | 196.2 | 16.8 | 61.0 | 38 | 1844 |
| J15 | WR | 183.2 | 195.0 | 17.0 | 61.0 | 40 | 1966 |
| J15 | RW | - | - | - | - | 38 | - |

* NRL Data

** Ref. 12

RESULTS AND DISCUSSION

Low cycle fatigue crack propagation studies were conducted with center-notched plate bend specimens loaded in full-reverse (balanced tension-compression) strain cycling. Specimen orientation resulted in fatigue crack propagation parallel to the principal or final rolling direction--in the ASTM designated weak fracture (WR) direction (8).

Data were taken in both normal room-temperature air and 3.5 percent salt water environments. Figure 13 is a log-log plot of fatigue crack growth rate data as a function of total strain range for 9Ni-4Co-0.25C steel of both rolling procedures (straight-rolled J14 and 1:1 cross-rolled J15). The open symbols denote air data and the closed symbols denote salt water data. Based on previous testing experience, several significant observations are evident from these data.

Consider first the air data which follow a straight-line plot on Fig. 13. The equation describing this power-law relationship is as follows:

$$\frac{d(2a)}{dN} = c(\epsilon_T)^n$$

where

2a = total crack length
N = cycle of repeated load

$$\frac{d(2a)}{dN} = \text{fatigue crack growth rate}$$

ϵ_T = total strain range
n = numerical exponent
c = numerical constant

The 6:1 slope (n=6) of this relationship is unusually steep for martensitic structural steels. This slope is indicative of the sensitivity of fatigue crack growth rates to changes in the level of cyclic strain. Previous results from HY-80, 5Ni-Cr-Mo-V, and 12% Ni maraging steels (2, 4, 12-14) show that a 4:1 slope is common for these martensitic steels. Exceptions to this rule occur among high YS, low fracture toughness, environmentally sensitive steels such as D6AC and 4335 (3). Steels of this type follow an approximate 4:1 slope at low cyclic strain levels, but exhibit

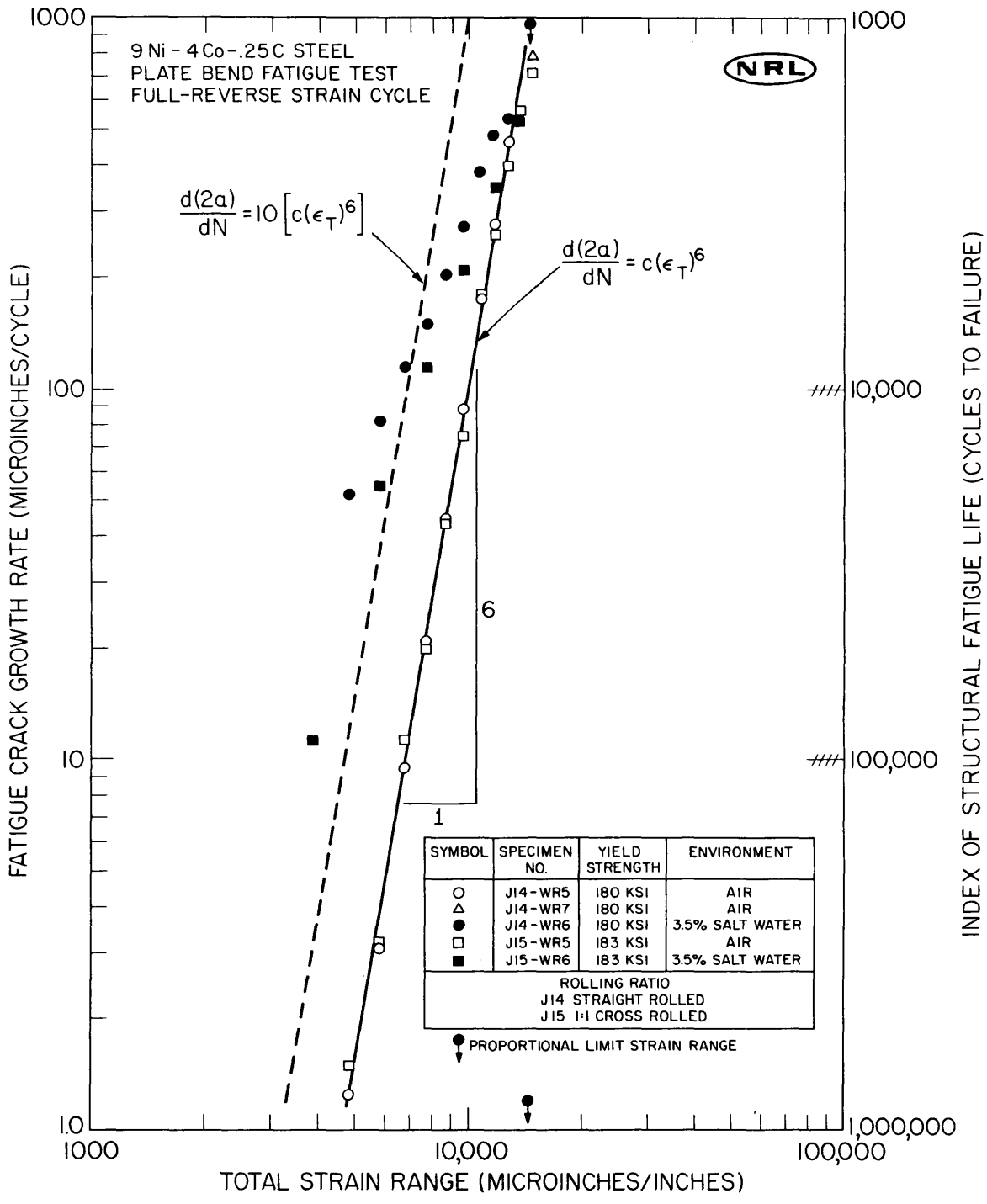


Fig. 13 - Log-log plot of fatigue crack growth rate versus total strain range for 9Ni-4Co-0.25C steel in air and 3.5 percent salt water.

a distinct transition point above which the slope becomes much steeper. Electron fractography studies have revealed that such a transition corresponds to a change in fracture mode from stepwise fatigue to a lower energy fracture mode (19). No such transition was observed in these tests on 9Ni-4Co-0.25C steel; the 6:1 slope was consistent over the entire span of the data. Consequently, in this regard, 9Ni-4Co-0.25C steel does not readily fall into any previously observed behavior pattern for a high strength steel.

Data were taken for total strain range values up to the elastic limit of the material, as indicated by the symbol for the proportional limit strain range on Fig. 13. In spite of the previously discussed 6:1 slope, the fatigue crack growth rate at the proportional limit strain range does not exceed 1000 microinches/cycle. This has been found to be a favorable bench mark among high strength steels.

Looking now at the salt water data, the effect of this highly aggressive environment on fatigue crack growth rates can be seen by the displacement of these data above the corresponding air data. The dashed line on Fig. 13 indicates the locus of an order of magnitude increase in fatigue crack growth rates. This line serves as a first order approximation of corrosion fatigue characteristics. Salt water data which exceed an order of magnitude increase are looked upon as indicating unfavorable material performance, and data which fall below this bench mark are viewed as favorable performance.

The observation that at higher total strain range levels the salt water data fall well below an order of magnitude increase and tend to converge with the air data is a highly favorable trend for this material. Such behavior is in contrast to the older generation of high strength steels, such as 4335 (3), which are known to be very sensitive to wet environments. The salt water fatigue crack growth rate data in these older steels diverges from the corresponding air data, leading to catastrophic rates of crack extension.

At lower cyclic strain levels, the increases in fatigue crack growth rates due to the salt water environment exceed an order of magnitude. This amounts to a rather severe reduction in fatigue crack propagation resistance

and indicates a serious potential for premature structural failure at relatively low cyclic strain levels in the presence of an aggressive environment. However, it is necessary to keep in mind that these data were taken at a loading rate of approximately five cycles/minute and that rate effects can possibly alter this curve.

Based on comparisons with other martensitic steels tested under identical conditions, this 9Ni-4Co-0.25C steel possesses wet fatigue characteristics which compare favorably with other "new" high strength steels, such as 5Ni-Cr-Mo-V (2) and 12% Ni maraging steels (4). The wet fatigue characteristics of these "new" steels are notably superior to the "old" high strength steels, such as D6AC and 4335 (3).

The two samples of 9Ni-4Co-0.25C steel tested in this study possess wide differences in anisotropy due to rolling. Since it is unlikely that premium quality material of this type would be employed structurally in the straight-rolled condition, these comparisons are somewhat academic. However, it is worthwhile to study the data in Fig. 13 with these differences in mind.

In air no consistent or significant differences were noted in fatigue crack growth rates between the two materials. This is in agreement with previous results on HY-80 (12) and 5Ni-Cr-Mo-V steels (2). In salt water the highly cross-rolled material was consistently superior by approximately 50 percent on crack growth rate. Previous studies on Ni-Cu alloys (16) had indicated some improvement in wet fatigue properties with rolling direction, but these are the most pronounced differences yet seen by the authors.

EVALUATION AND CONCLUSIONS

A comparative evaluation of the low cycle fatigue crack propagation characteristics of 9Ni-4Co-0.25C steel is shown in Fig. 14, which is a log-log plot of fatigue crack growth rate versus the ratio of total strain range to proportional limit strain range. This graph shows the air environment fatigue crack propagation curves for 9Ni-4Co-0.25C steel and five other martensitic high strength structural steels on a strain range basis normalized with respect to elastic strength level.

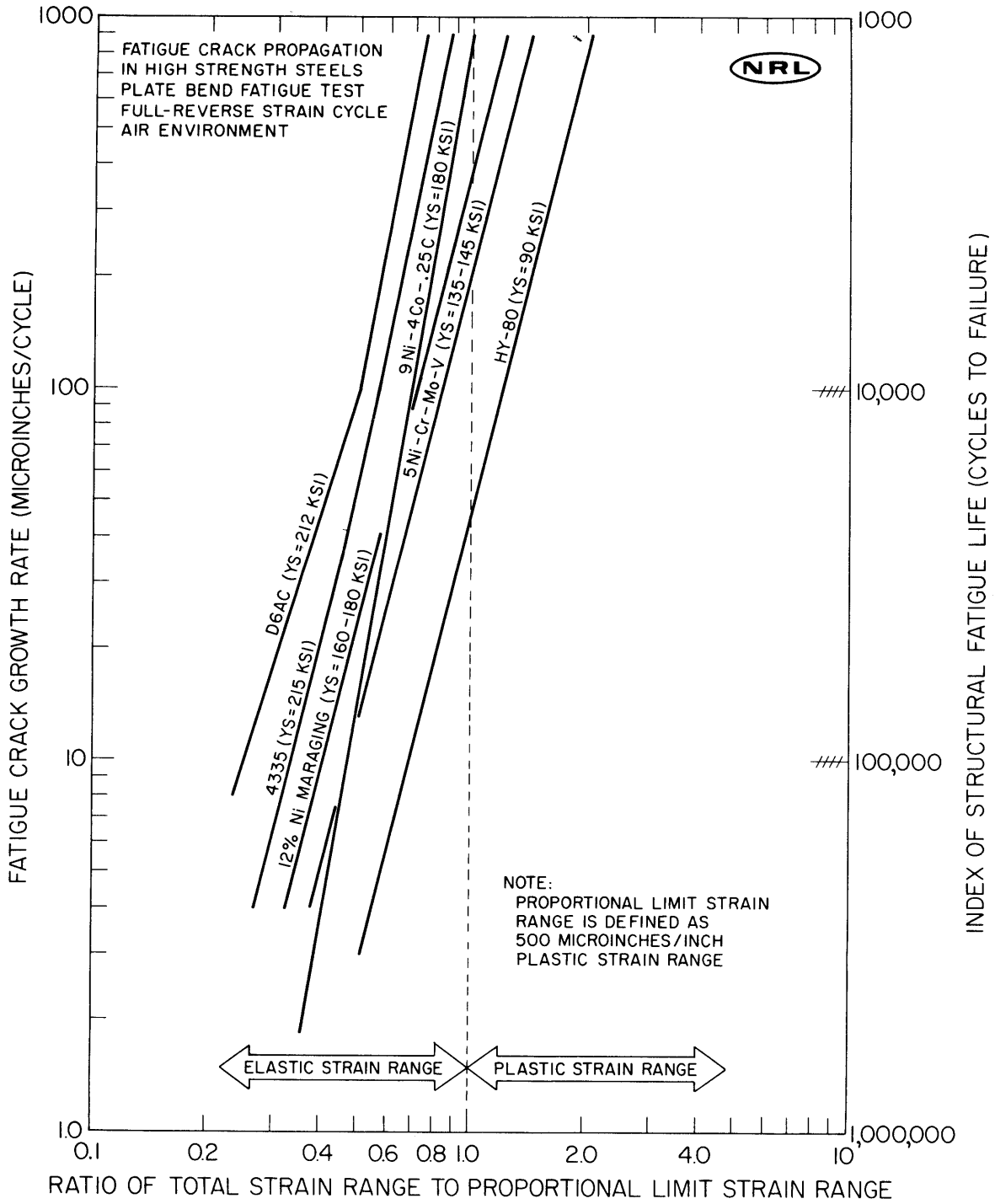


Fig. 14 - Log-log plot of fatigue crack growth rate versus the ratio of total strain range to proportional limit strain range for a variety of high strength structural steels.

Figure 14 indicates that at nominal cyclic strain levels in the usable range, from 50 to 100 percent of elastic strength, the "new" generation of high strength structural steels (5Ni-Cr-Mo-V, 12% Ni maraging, and 9Ni-4Co-0.25C) will propagate fatigue cracks more rapidly than HY-80 but slower than the "old" generation of high strength steels (4335 and D6AC). These distinctions are largely due to differences in strength level. However, in the case of 4335 and D6AC, low fracture toughness and environmental sensitivity add to the reduction in fatigue crack propagation resistance.

Among the "new" steels, it can be seen that the steep slope of the 9Ni-4Co-0.25C curve places this material in a less favorable position at critical strain range values above 70 percent of proportional limit loading. In this strain range region, its fatigue crack propagation characteristics depart significantly from the established pattern for the "new" steels and more closely approach the characteristics of the "old" steels.

Based on the data from this series of tests on 9Ni-4Co-0.25C steel, the following conclusions are evident:

1. In an air environment, the low cycle fatigue crack propagation characteristics of 9Ni-4Co-0.25C steel, quench-and-temper heat treated to a YS of 180 ksi, are less favorable than other competitive "new" high strength martensitic structural steels, but are somewhat improved over the "old" high strength steels.
2. In a 3.5 percent salt water environment, the low cycle fatigue crack propagation characteristics of this material are comparable with other "new" high strength martensitic steels and are considerably superior to the salt water fatigue performance of the "old" high strength steels.

STRESS CORROSION CRACKING
STUDIES OF SOME HIGH STRENGTH METALS
(R.W. Judy, Jr. and R.J. Goode)

Aqueous stress corrosion cracking studies have been conducted on a variety of high strength titanium alloys, aluminum alloys and steels. The tests were conducted using the cantilever method introduced by B.F. Brown (20).

A number of steels, titanium alloys and aluminum alloys are sensitive to stress-corrosion-cracking (SCC) which is conveniently expressed in terms of K_I , the stress intensity factor. A threshold level of stress intensity, denoted $K_{I_{SCC}}$, above which SCC will definitely occur, has been shown to exist for many of these environmental sensitive materials (20, 21). Comparison of $K_{I_{SCC}}$ with K_{I_X} , the "dry" stress intensity factor, gives an indication of the relative sensitivity of an alloy to the aqueous environment. The formula used in the SCC studies was the cantilever equation:

$$K_I = \frac{4.12M\sqrt{1 - \alpha^3}}{BD^{3/2}}$$

where M = moment at the test section
 B = specimen width
 D = specimen depth
 $\alpha = 1 - \frac{a}{D}$
 a = depth of flaw (notch and fatigue crack)

SCC OF SOME TITANIUM ALLOYS

The titanium specimens cut from 1-in.-thick plate were 1/2x1x7-in.-long with a machined notch and fatigue crack flaw located at the center so that the fracture orientation was in the WT or LT fracture direction (8), through the 1-in. dimension. The specimens had 1/32-in. side grooves to suppress shear lip formation. A 3.5 percent salt water solution was used as the aqueous environment.

The SCC data, along with some mechanical properties of the alloys tested, are shown in Table 13 and Figs. 15 through 21. In addition, results of SCC studies of a MIG weld of Ti-6Al-2Cb-1Ta-0.8Mo are shown in Table 14 and Fig. 22. Except as noted, all materials tested were in the as-received condition.

Stress-corrosion-cracking studies of Ti-6Al-4V showed that alloy T-95 (0.12 wt-% O₂) and $K_{I_{SCC}}/K_{I_X}$ values of 68/94. Comparing these values with other Ti-6Al-4V alloys previously tested (4) (T-91, 0.08 wt-% O₂, $K_{I_{SCC}}/K_{I_X} = 90/118$; and T-32, high interstitial, $K_{I_{SCC}}/K_{I_X} = 80/101$) showed no real correlation between SCC behavior and O₂ content.

TABLE 13
MECHANICAL AND SCC PROPERTIES OF SOME TITANIUM ALLOYS

| Alloy No. | Nom. Comp. | YS (ksi) | DWTT (ft-lb) | $K_{I,x}$ (ksi \sqrt{in}) | $K_{I,sc}$ (ksi \sqrt{in}) | Remarks |
|-----------|---------------------|----------|--------------|------------------------------|-------------------------------|----------------------------------|
| T-41 | Ti-6Al-6Zr-1Mo | 102 | 2646 | 106 | 102 | |
| T-52 | Ti-3Al | 71.3 | >5000 | 81 | 64 | |
| T-69 | Ti-10Mo-5.4Sn | 115 | 1905 | 129 | 128 | 1200°F/48 hr/WQ |
| T-94B | Ti-7Al-2.5Mo | | 2086 | 118 | 93 | 1800°F/1 hr/He Cool |
| T-95 | Ti-6Al-4V | | 811 | 94 | 68 | ELI Grade (0.12 O ₂) |
| T-96 | Ti-6Al-2Cb-1Ta-.8Mo | | 2384 | 117 | 98 | |
| T-97 | Ti-11Mo-5Sn-5Zr | | 1021 | 117 | 94 | |

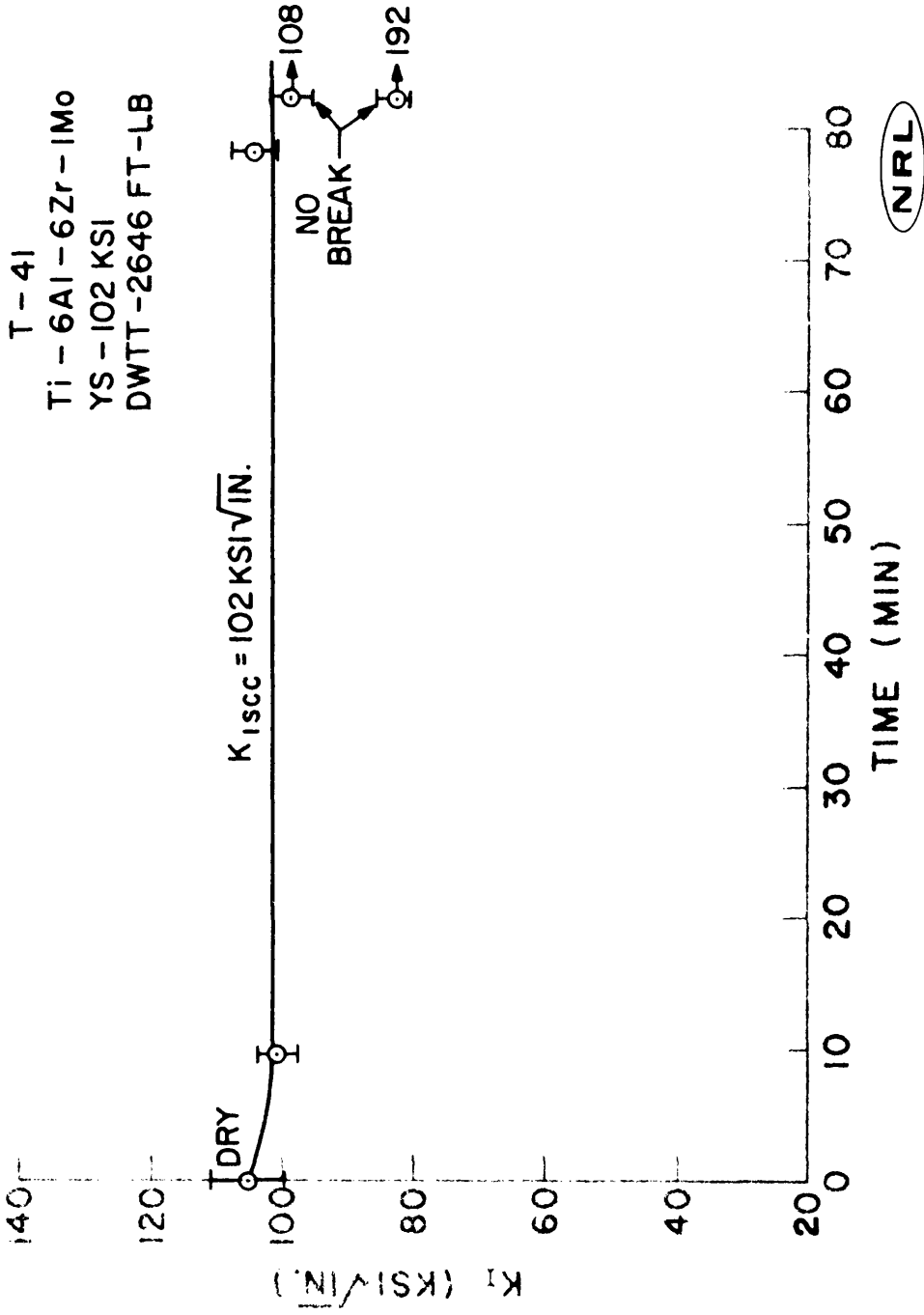


Fig. 15 - Stress-corrosion-cracking characteristics of Ti-6Al-6Zr-1Mo alloy (T-41).

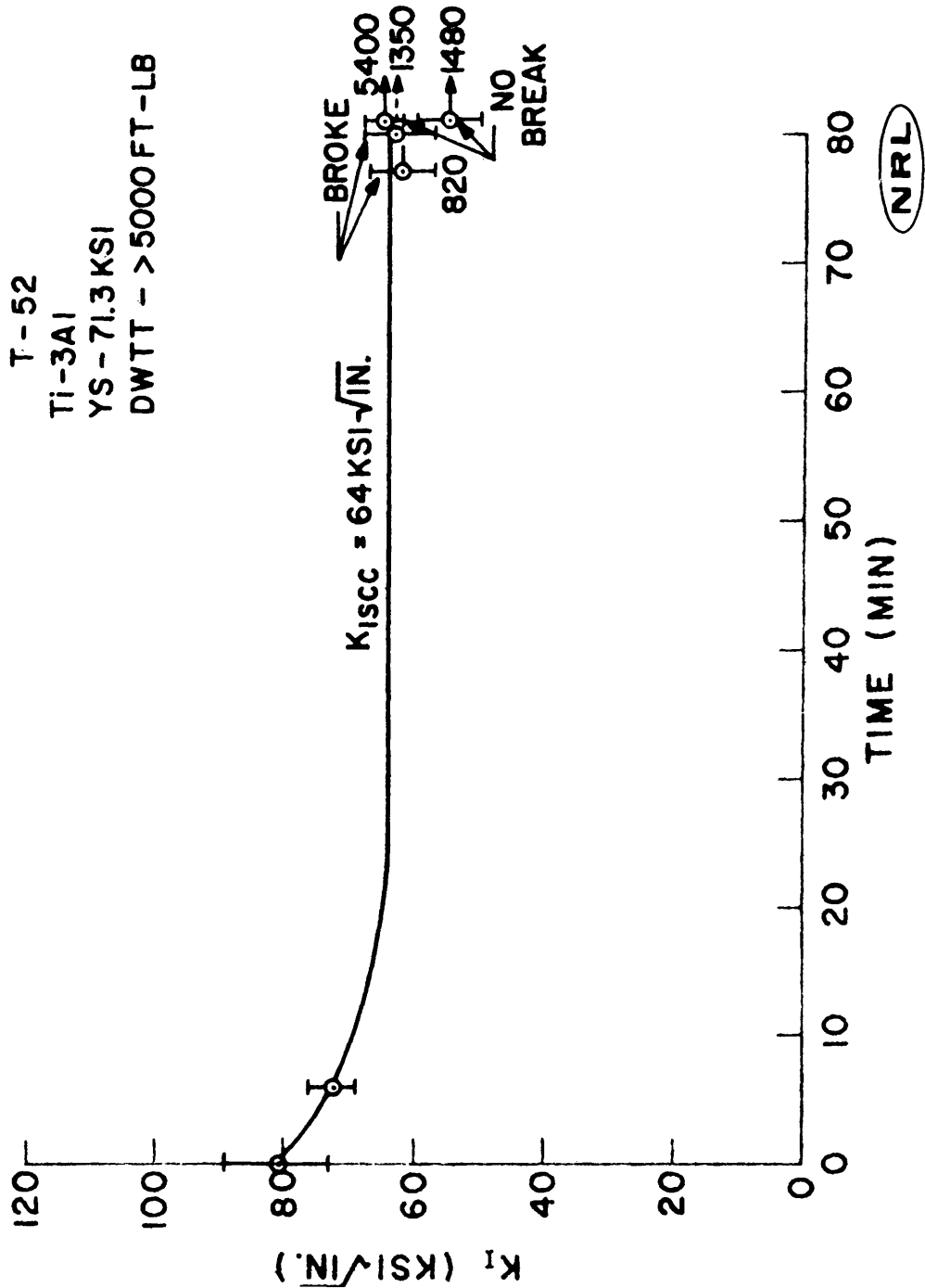


Fig. 16 - Stress-corrosion-cracking characteristics of Ti-3Al alloy (T-52).

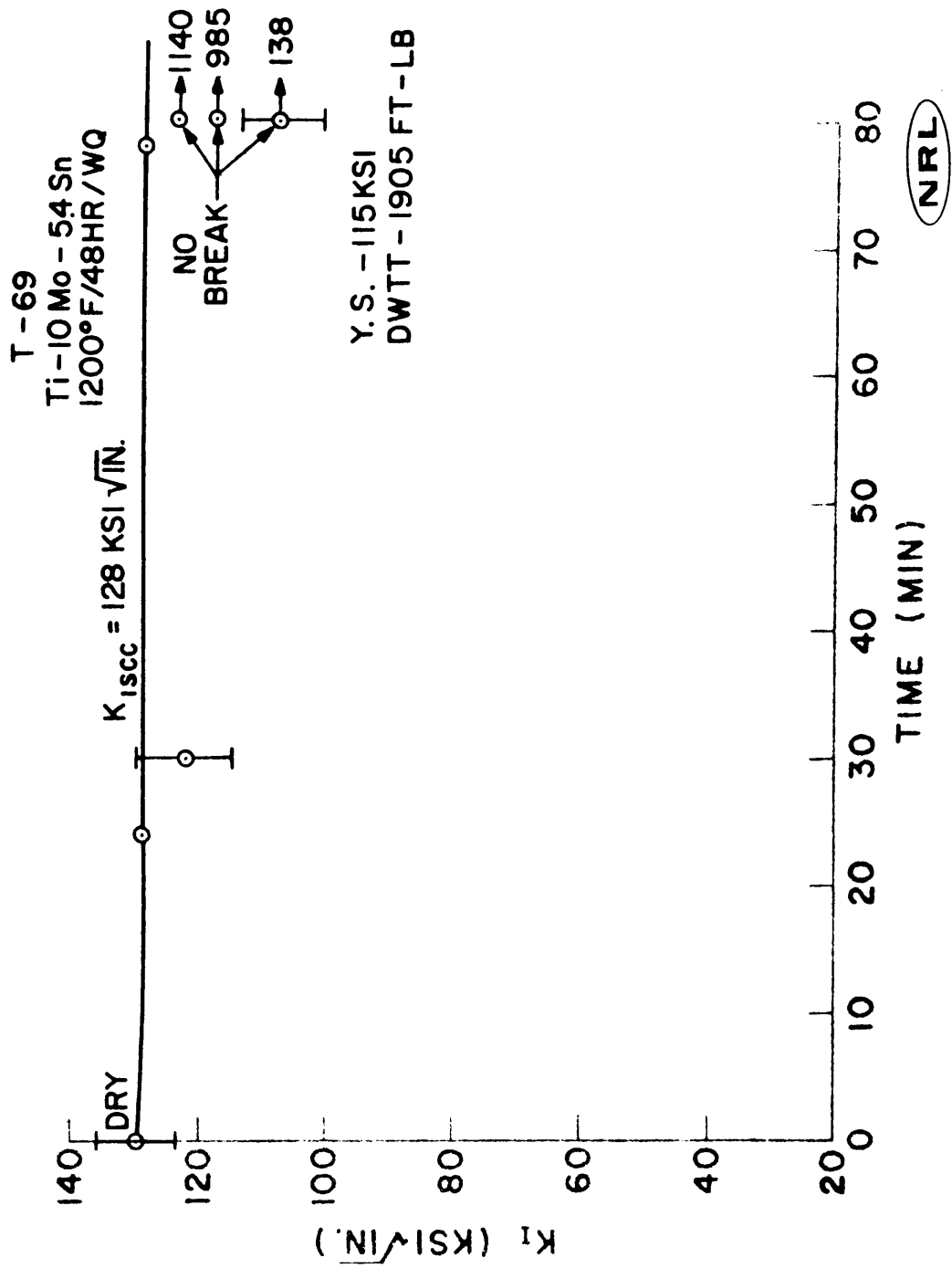


Fig. 17 - Stress-corrosion-cracking characteristics of Ti-10Mo-5.4Sn alloy (T-69).

T-94 B
 Ti-74I-2.5Mo
 1800°F/1HR/He COOL
 DWTT - 2086 FT LB

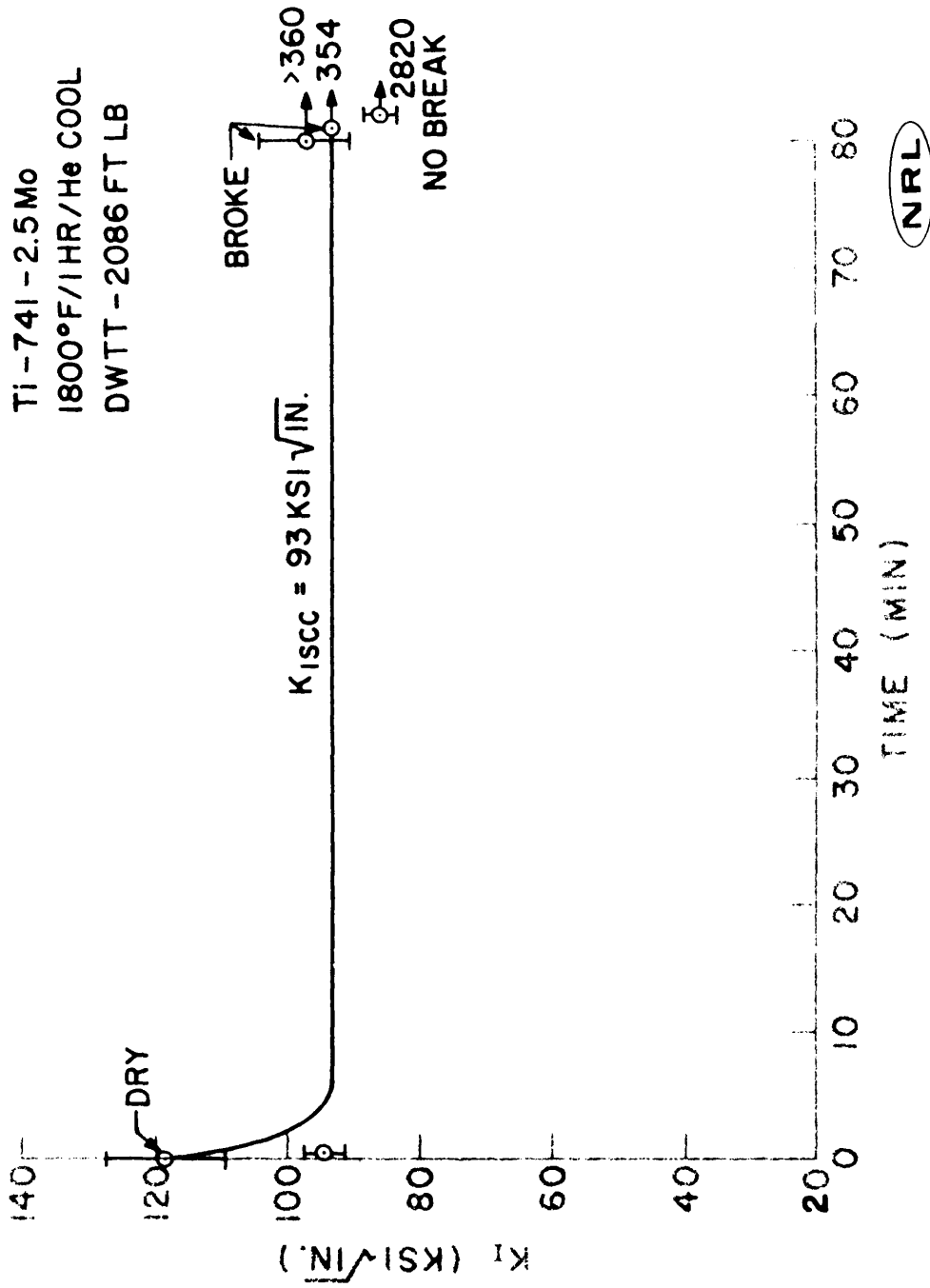


Fig. 18 - Stress-corrosion-cracking characteristics of Ti-74Al-2.5Mo alloy (T-94B).

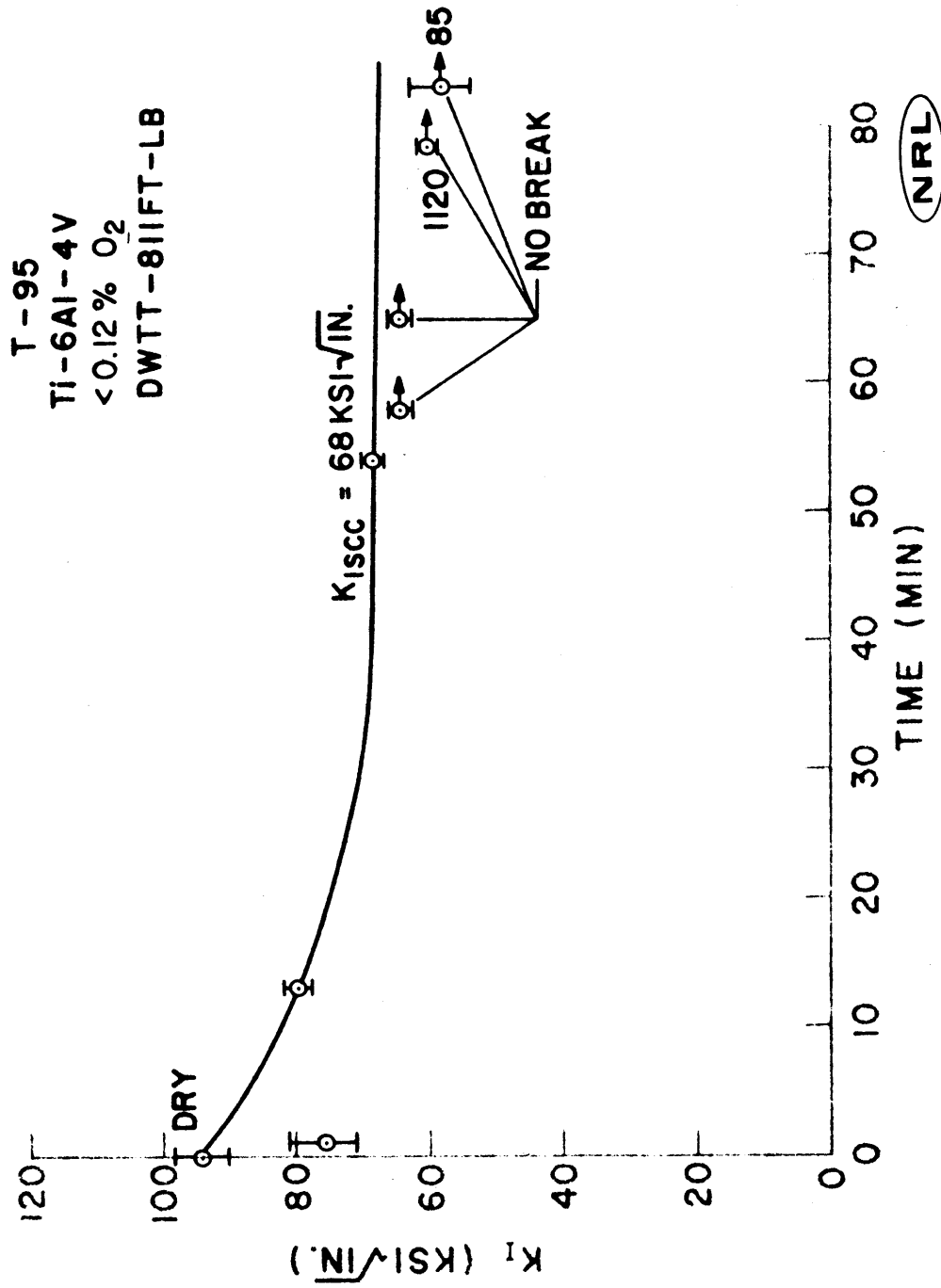


Fig. 19 - Stress-corrosion-cracking characteristics of Ti-6Al-4V alloy (T-95).

T-96
 Ti-6Al-2Cb-1Ta-.8Mo
 DWTT - 2384 FT-LB

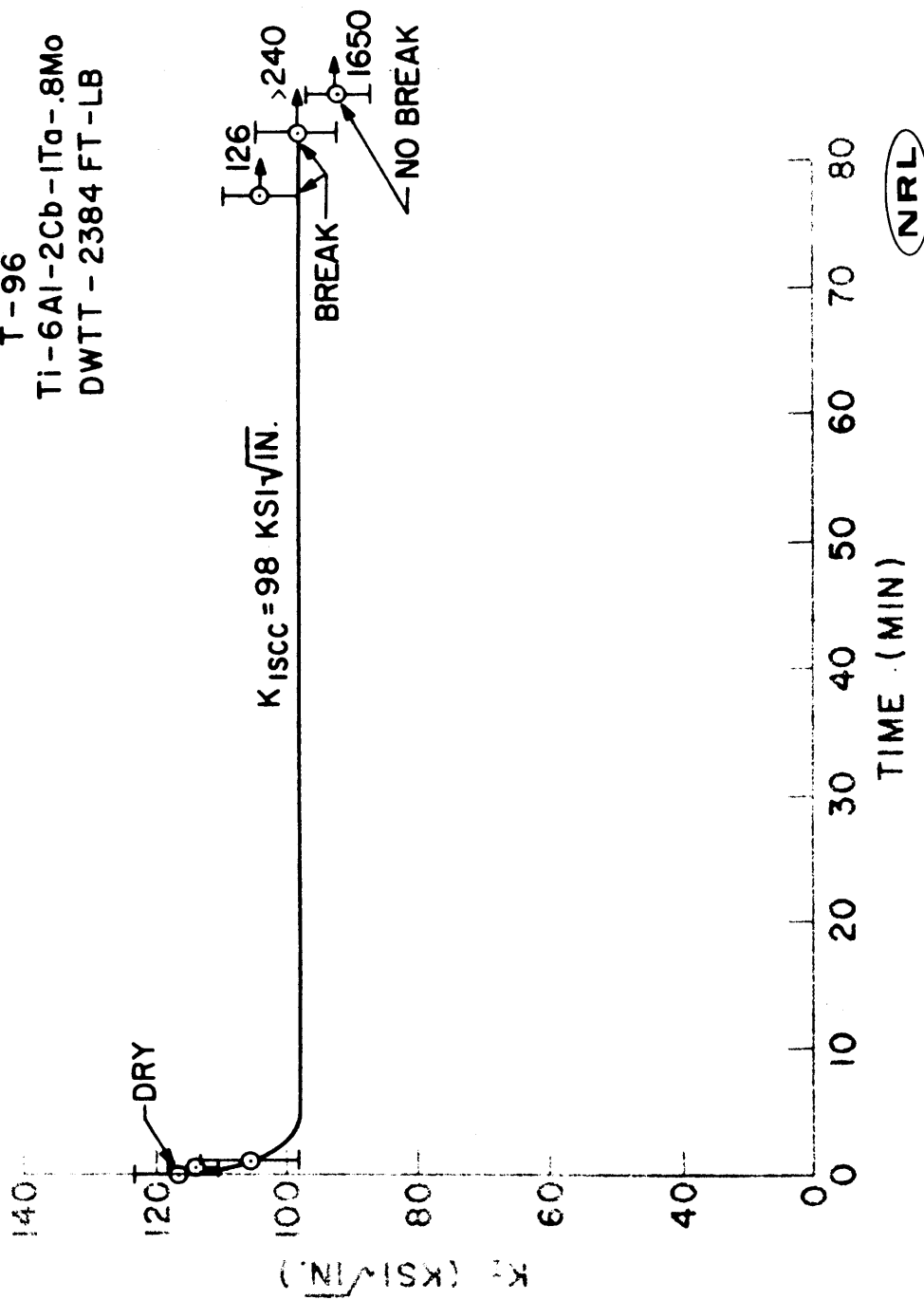


Fig. 20 - Stress-corrosion-cracking characteristics of Ti-6Al-2Cb-1Ta-.8Mo alloy (T-96).

T-97
 Ti-11Mo-5Sn-5Zr
 DWTT - 1021 FT-LB

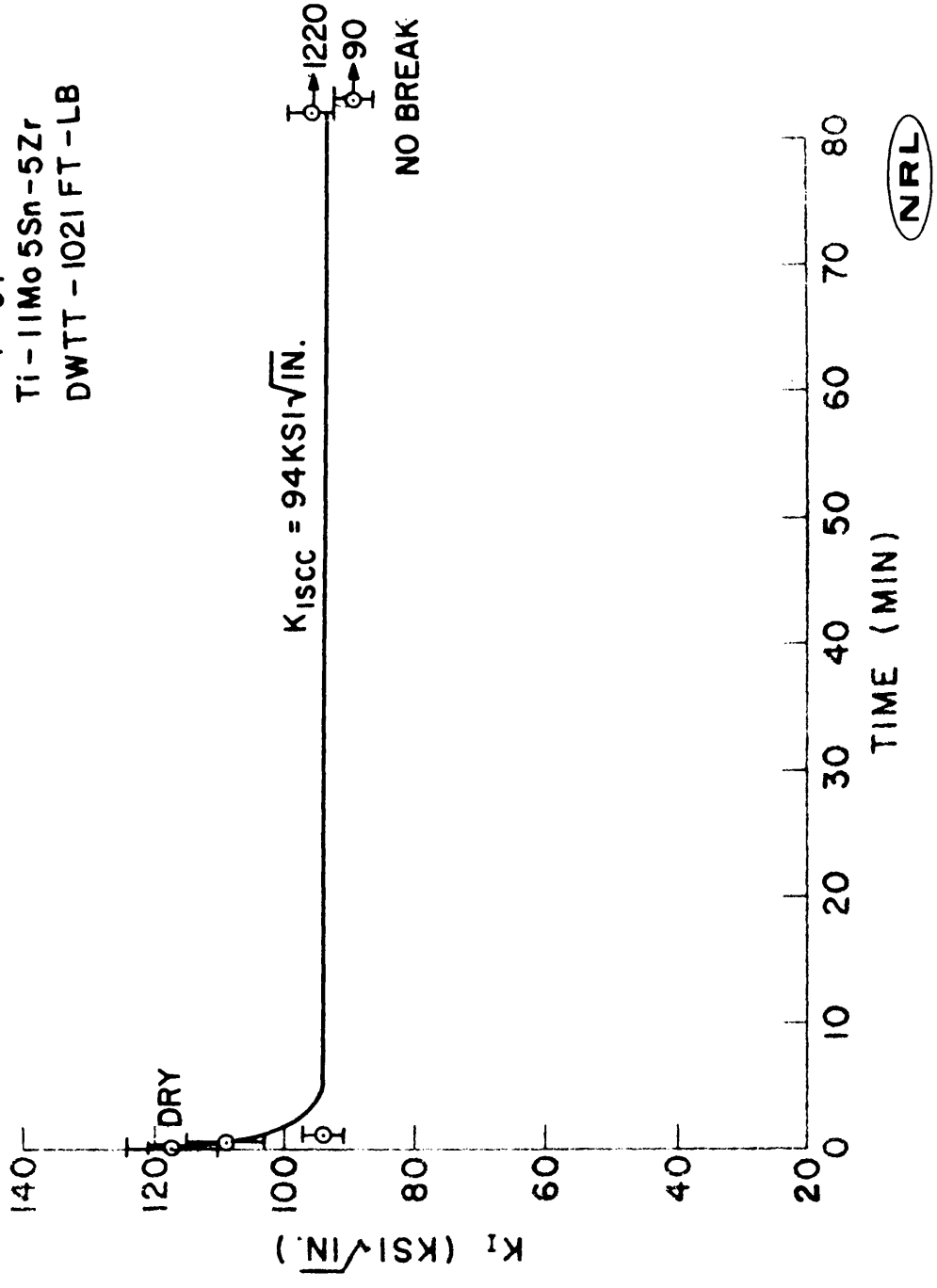


Fig. 21 - Stress-corrosion-cracking characteristics of Ti-11Mo-5Sn-5Zr alloy (T-97).

TABLE 14

T96 MIG WELD

| Spec. No. | K_1 (ksi/in) | K_2 (ksi/in) | Time (min) | Env | $K_{1\Delta}$ (ksi/in) | $K_{2\Delta}$ (ksi/in) | Remarks |
|-----------|-------------------|-------------------|---------------|-----|---------------------------|---------------------------|--------------------|
| 1 | 90 | 100 | 1/2 | SW | 109 | 112 | Weld ϵ |
| 2 | 85 | 94 | 1 | SW | 103 | 113 | Weld ϵ |
| 3 | 84.3 | 95.7 | 1 | SW | - | - | Weld ϵ |
| 4 | 81 | 76 | 1 | SW | 98 | 103 | $\epsilon + 1/8"$ |
| 5 | 87 | 87 | 28 | SW | - | - | $\epsilon + 1/8"$ |
| 6 | 75 | 79 | 1/2 | SW | 90 | 95 | $\epsilon + 3/16"$ |
| | | NO BREAK | | | | | |
| 1 | 87 | 97 | 66 | SW | | | |
| 6 | 71 | 74 | 61 | SW | | | |

Base Plate
 $K_{Ix} = 117$
 $K_{Isc} = 98$

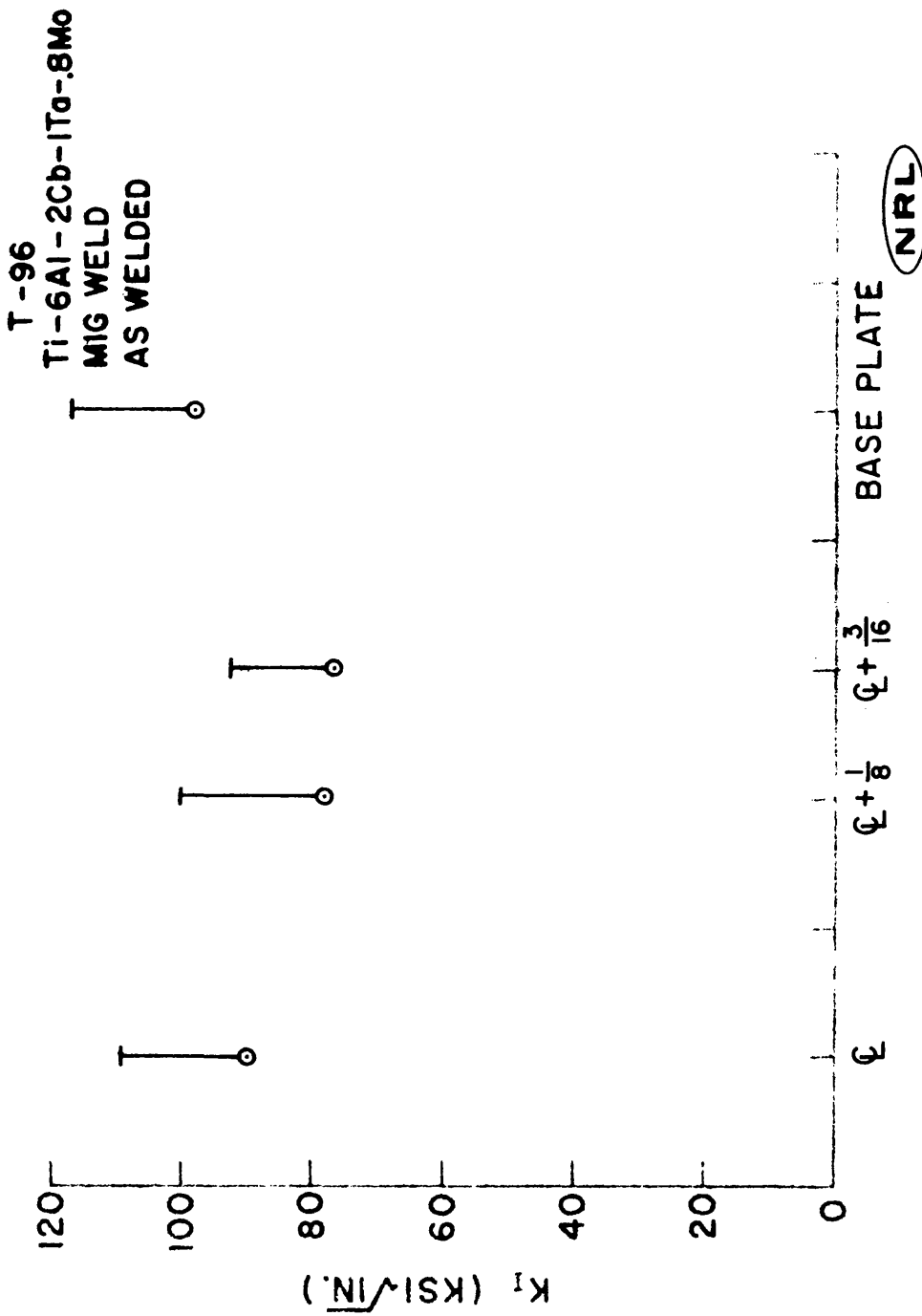


Fig. 22 - Stress-corrosion-cracking characteristics of a MIG weldment in a 1-in.-thick plate of Ti-6Al-2Cb-1Ta-0.8Mo (T-96). Base plate characteristics are shown for reference.

The beneficial effect of molybdenum additions can be noted on results of SCC tests on alloy T-96, Ti-6Al-2Cb-1Ta-.8Mo which represented the substitution of 0.8% Mo for 1% Al in Ti-7Al-2Cb-1Ta an alloy which is known to be quite sensitive to SCC (4, 20). The T-96 alloy was not sensitive, having $K_{I_{SCC}}/K_{I_X} = 98/117$ in the mill-annealed condition.

Stress-corrosion-cracking tests were conducted on a limited number of samples of the MIG weldment of 1-in. plate of T-96, Ti-6Al-2Cb-1Ta-0.8Mo described in the titanium fracture toughness section of this report. Since the amount of material was limited, specimens were notched at the weld centerline and at 1/8-in. and 3/16-in. from the weld centerline to get some feel of heat-affected-zone (HAZ) SCC resistance. The results of this study are shown in Table 14 and Fig. 22. No specimens were tested in the "dry" environment; in place of K_{I_X} , the dry stress intensity factor was calculated from the additional flaw size generated by the stress-corrosion crack, and is denoted as $K_{I\Delta}$. This method of obtaining the dry K_I has been shown valid by Brown (21). The specimens were all step-loaded until they broke, $K_{I_{SCC}}$ being taken as the lowest "wet" K_I value obtained.

The data showed a slight decrease in both $K_{I\Delta}$ and $K_{I_{SCC}}$ in the weld-plus-HAZ compared to results at the weld centerline. All values attained from the welded specimens were lower than base plate values.

SHORT-TERM SCC OF HY-130/150 PLATE AND A 9Ni-4Co-0.25C WELDMENT

Short-term stress-corrosion studies of 1-in.-thick plate of HY-130/150 steel (coded H98) and a weldment of 9Ni-4Co-0.25C steel were conducted. The test times were rather limited due to lack of facilities for long-term investigations.

Specimens of HY-130/150 were tested in the as-rolled condition and in the stress-relieved condition. The specimens were 1/2x1x7-in. long and were side-grooved to suppress shear lip formation. The results of these tests are shown in Figs. 23 and 24. A slight SCC susceptibility was shown by the small decrease of K_I due to the salt water. It should be emphasized that

H-98
 HY 130 - 150
 AS REC'D

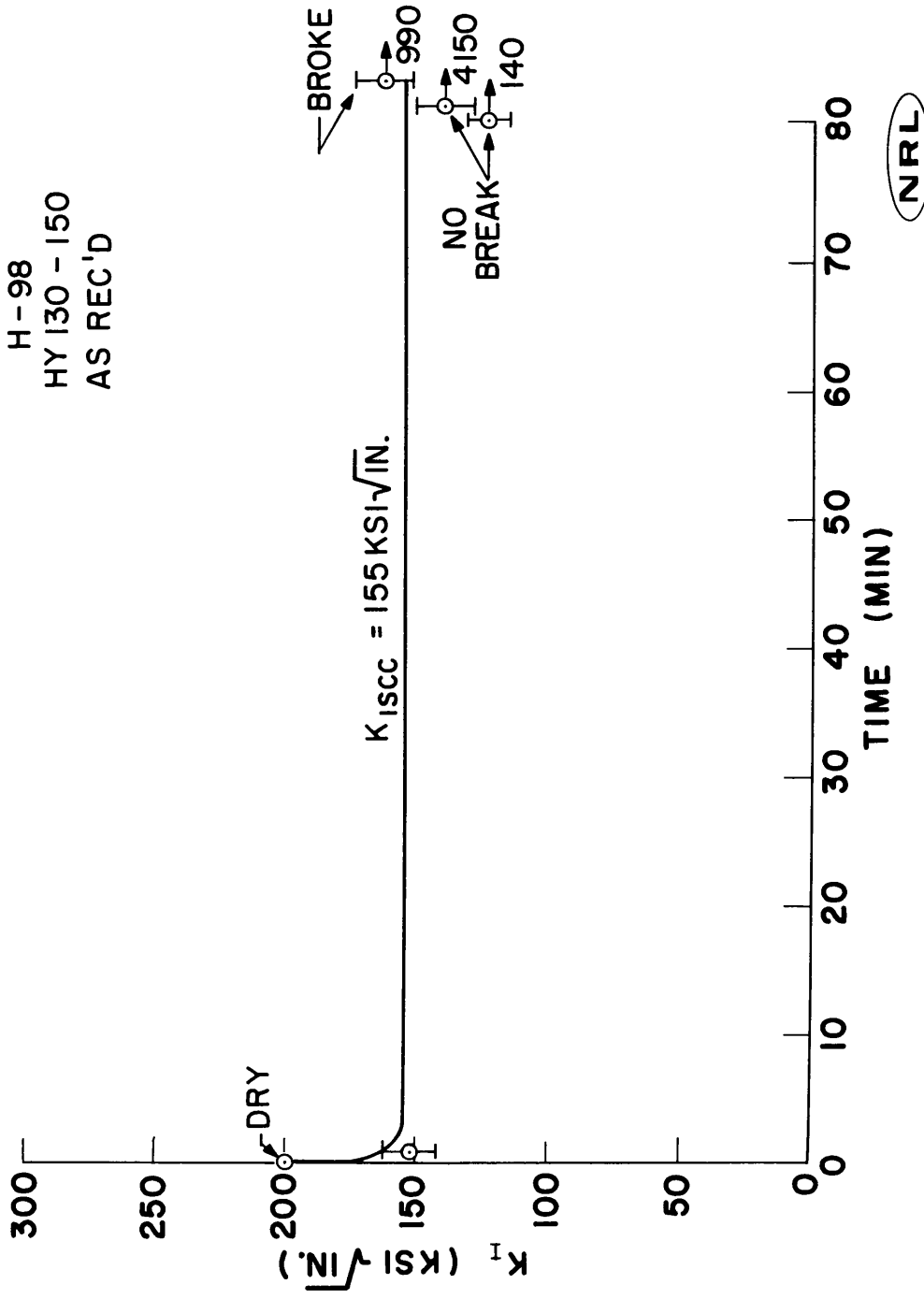


Fig. 23 - Stress-corrosion-cracking characteristics of HY-130/150 steel in as-received condition.

H-98
 HY 130-150
 STRESS RELIEVED

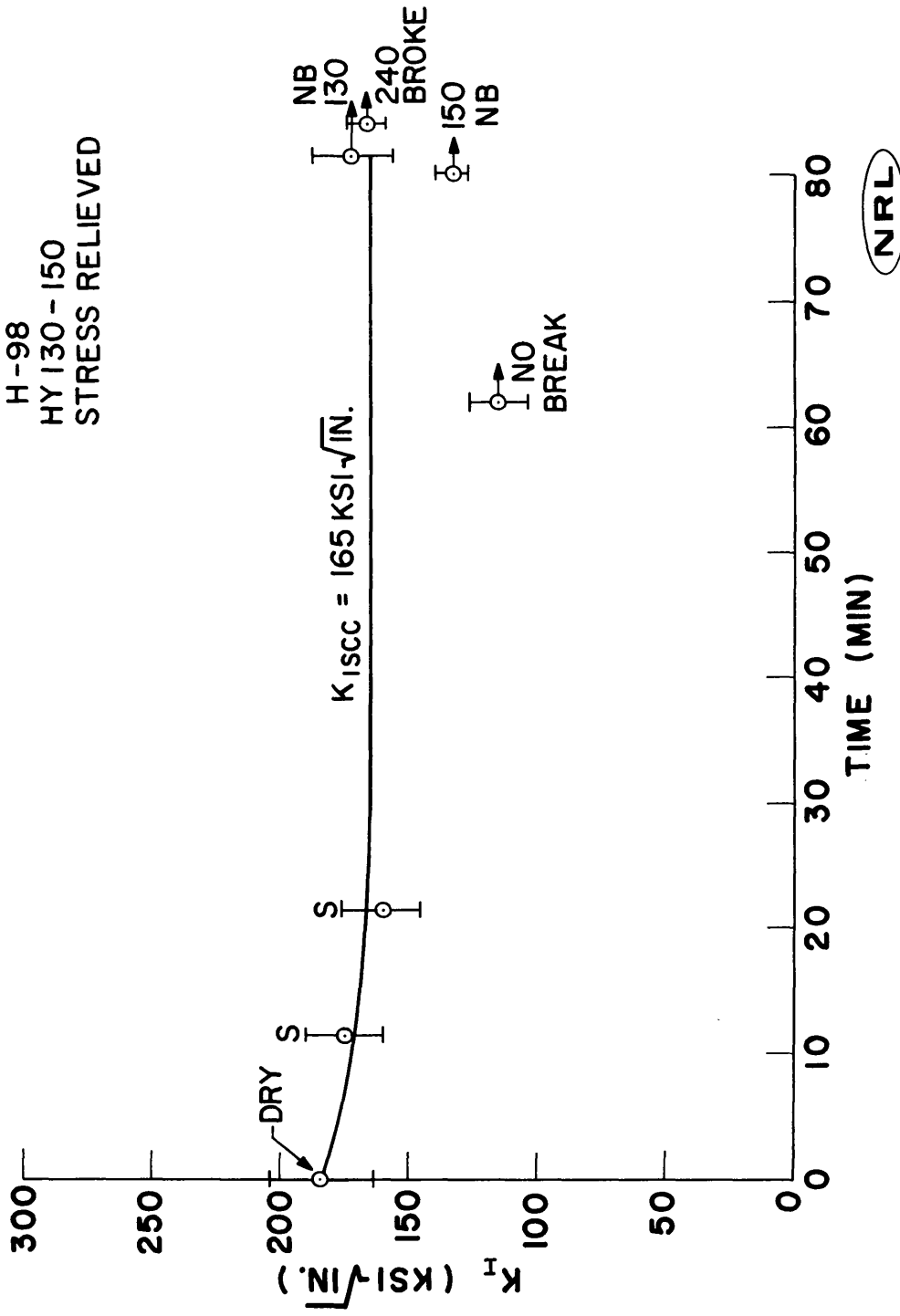


Fig. 24 - Stress-corrosion-cracking characteristics of HY-130/150 steel in stress-relieved condition.

the K_{I_X} or $K_{I_{SCC}}$ numbers shown do not represent valid, absolute values due to specimen size effects (specimens wider than 1/2-in. are indicated to be required to satisfy necessary fracture mechanics conditions) and the limited times involved in testing each specimen. However, the tests do reveal that this steel shows some sensitivity to SCC. Values of $K_{I_{SCC}}/K_{I_X} = 155/200$ and $K_{I_{SCC}}/K_{I_X} = 165/184$ were observed for the as-received and stress-relieved conditions, respectively, for this steel.

Results of the tests on the 9Ni-4Co-0.25C weldments are shown in Fig. 25. The test material was a standard "J" weldment of two 1-in. 9Ni-4Co-0.25C steel plates. The SCC properties of the weld centerline, various points in the heat-affected-zone (HAZ), and the base plate were determined. Since exact definition of each of these zones was impossible, specimens were notched at the weld centerline and at 1/8-in., 1/4-in., 3/8-in., 9/16-in., and 3/4-in. from the centerline to provide a profile of the SCC characteristics across the weldment.

The specimen dimensions were 7-in. long by 3/4-in. wide for the specimens used in determining SCC properties at the weld centerline, the base plate properties, and the properties at 3/8-in. from weld centerline. Specimens notched at 1/8-in. and 1/4-in. from weld centerline were 7-in. long by 11/32-in. All specimens were side-grooved and fatigue cracked.

The profile of $K_{I_{SCC}}$ across the weld, HAZ, and base plate can be seen in Fig. 25. Values in the base plate and at weld centerline were obtained from several specimens; the values at 1/8-in. and 1/4-in. were obtained by steploading two specimens at each location.

A general decrease in the threshold SCC level can be seen between the weld and various points in the HAZ, and between the base plate and the weld.

Some difficulty was encountered during the tests when voids or particles were encountered in the test section. Either imperfection was sufficient to require extremely high loads to break the specimen and did not yield valid test data. Some of these are shown in Fig. 26.

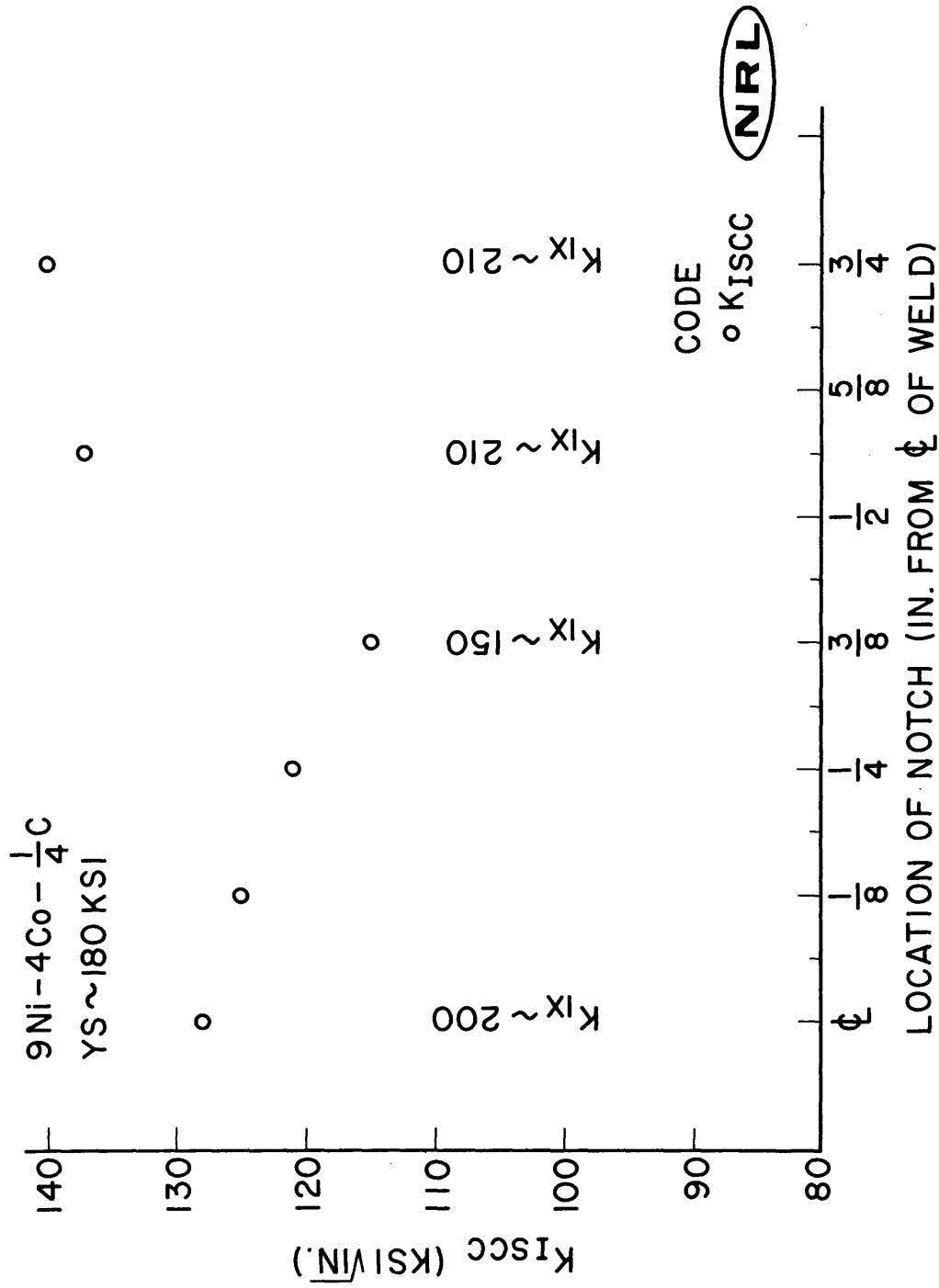


Fig 25 - Profile of stress-corrosion-cracking characteristics of 9Ni-4Co-0.25C weldments.

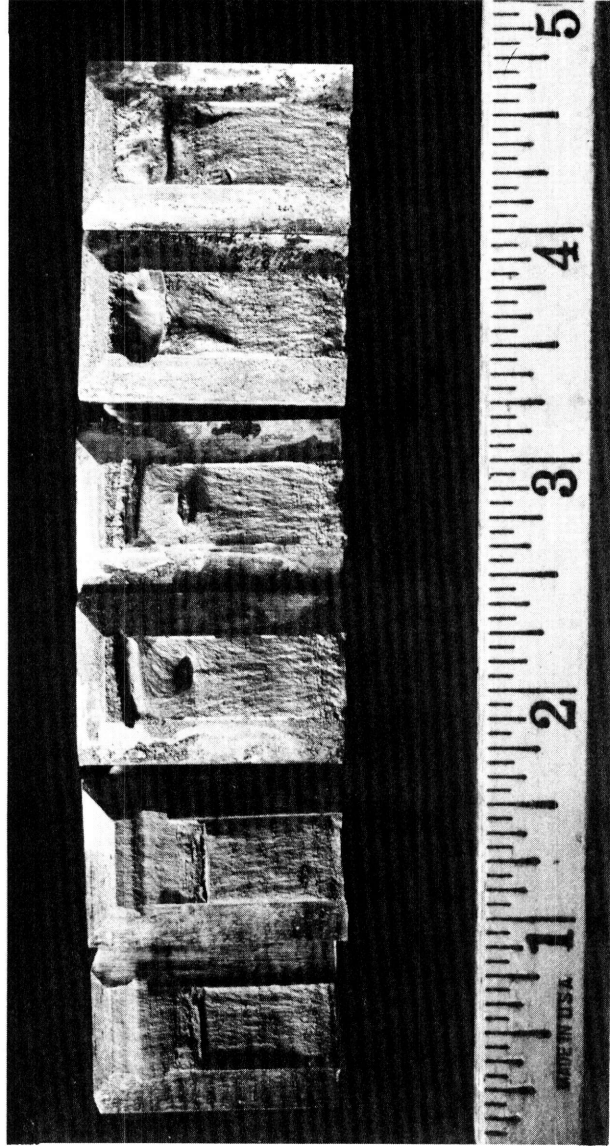


Fig. 26 - Fracture appearance of 9Ni-4Co-0.25C weldment.

PROPERTIES OF ALUMINUM ALLOYS

| Alloy | Code | YS (ksi) | DWTT (ft-lb) | K _{Ix} (ksi√in) | K _{Isc} (ksi√in) | Remarks |
|------------|------|-------------|-----------------|-----------------------------|------------------------------|-------------------|
| 2219T851 | A15 | 58.4 | 281 | 22.8 | 22 | |
| 7106T63 | A17 | 52.5 | 514 | 32.7 | 23 | |
| 7039-T6X31 | A18 | 51.6 | 573 | 28.3 | 11.5 | 6 in. thick plate |

NOTE:

YS and DWTT data for WR specimen orientation.
 SCC data for TW or short transverse orientation.

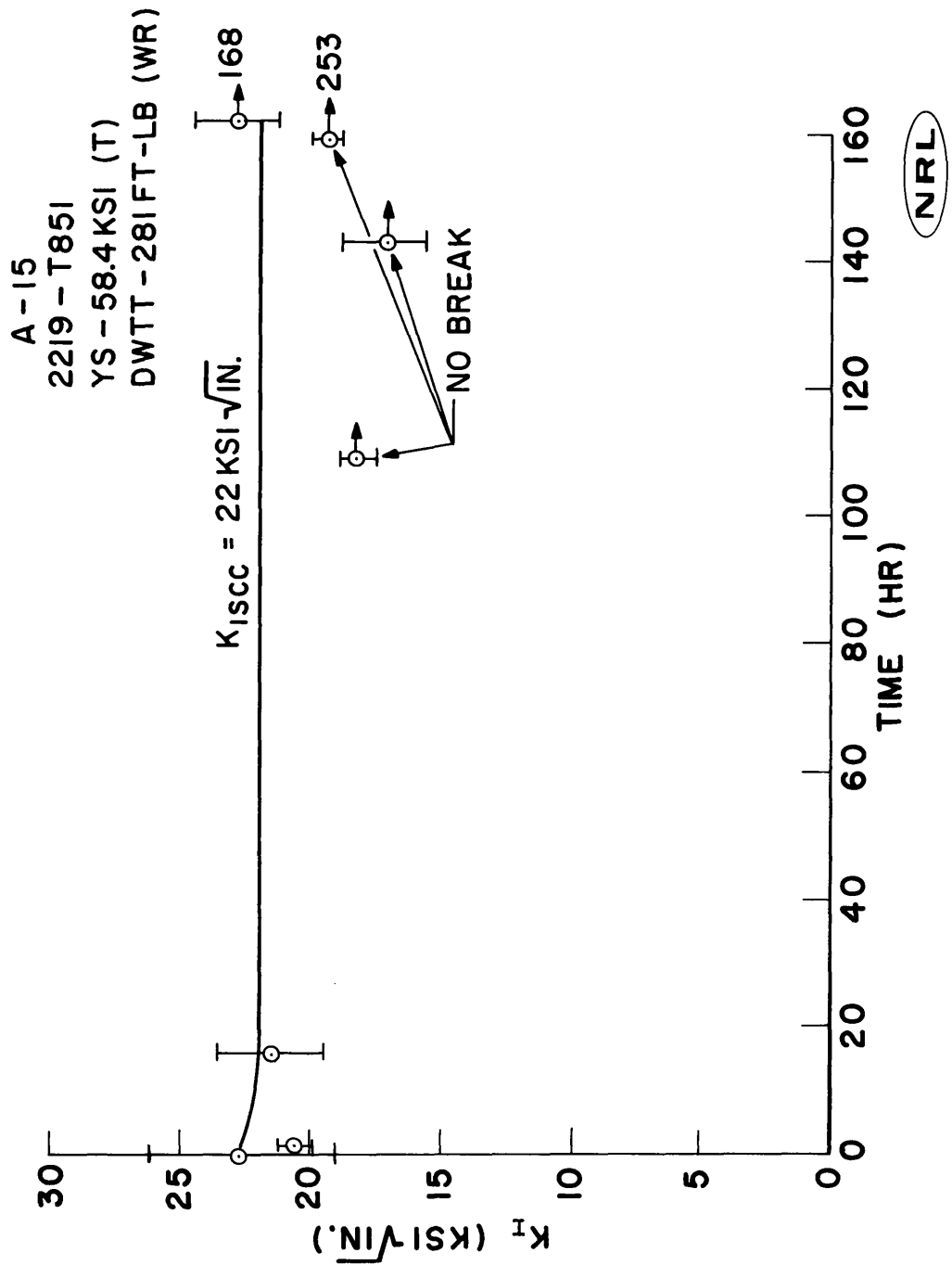


Fig. 27 - Stress-corrosion-cracking characteristics of 2219-T851 aluminum alloy.

A-17
 7106 - T63
 TW ORIENTATION
 YS - 52.5 KSI
 DWTT - 514 FT-LB

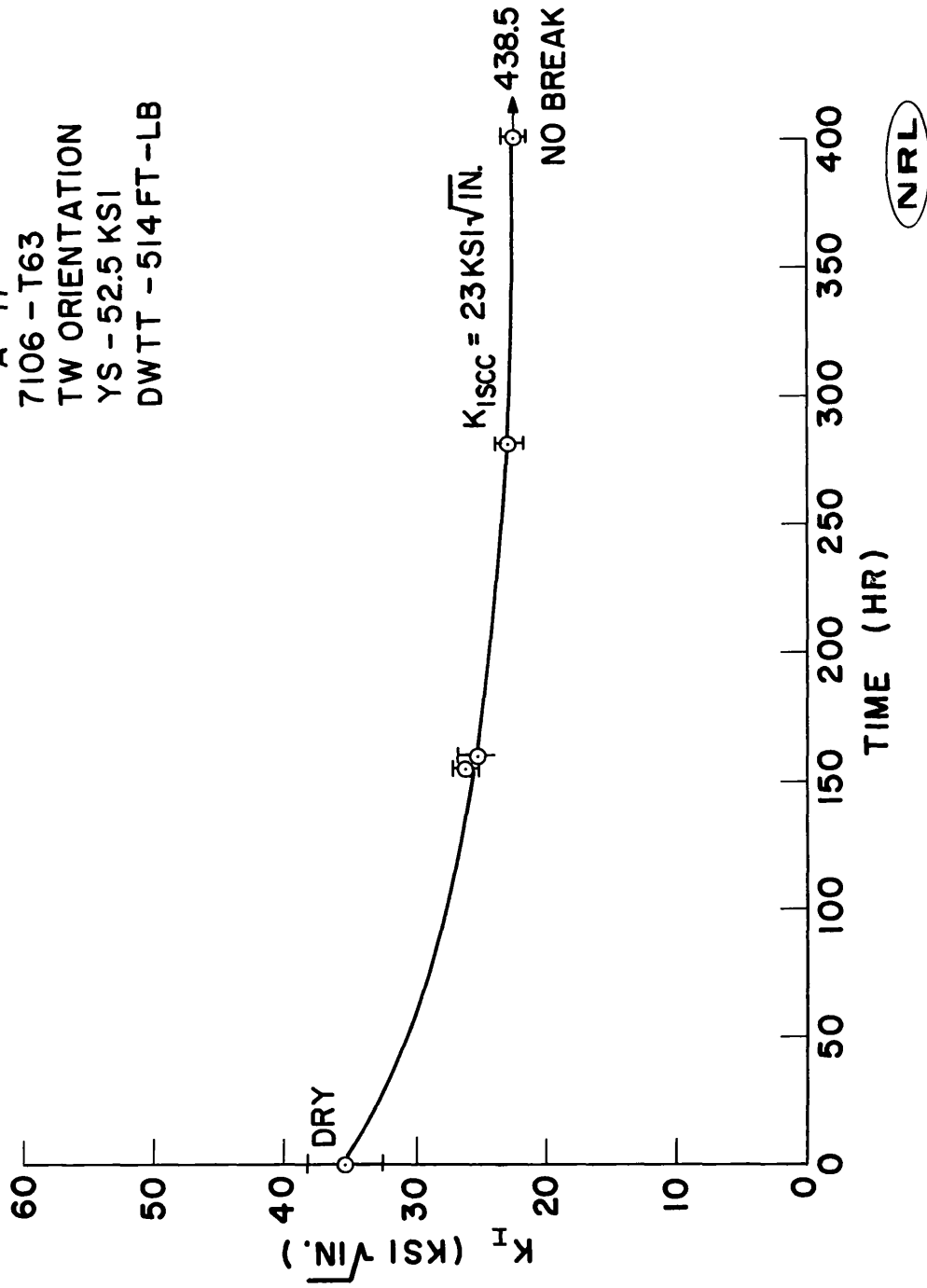


Fig. 28 - Stress-corrosion-cracking characteristics of 7106-T63 aluminum alloy.

A - 18
 7039 - T6X31
 YS 51.6 KSI
 DWTT 573 FT-LB

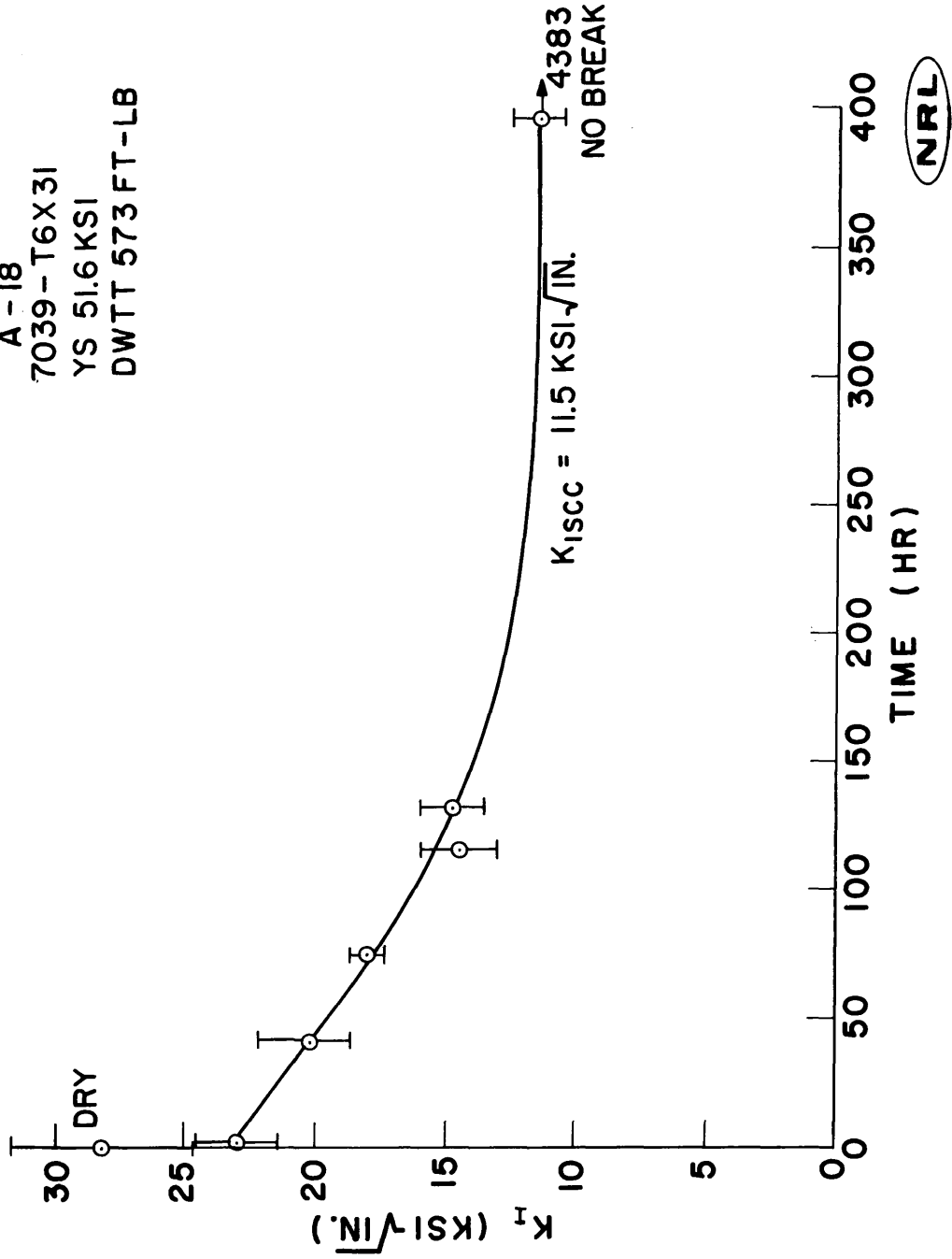


Fig. 29 - Stress-corrosion-cracking characteristics of 7039-T6X31 aluminum alloy.

The results of these tests are at best a general indication of whether or not the material is sensitive to environmental cracking. Due to the test methods used, a valid definitive number for K_{Isc} could not be determined. The results indicate some sensitivity to SCC.

SCC OF ALUMINUM ALLOYS

For aluminum alloys the short transverse fracture direction (TW) reveals the greatest sensitivity to SCC. Therefore specimens of several alloys were tested in this orientation. The specimens were obtained from 1-in.-thick plate by electron beam welding tabs to a block 1-in. square in cross-section. This technique was successful in some cases; in other cases, the weld or heat-affected-zone proved more sensitive to SCC than parent material.

Results of tests on 2219-T851, 7106-T63, and 7039-T6X31 are shown in Table 15 and Figs. 27-29. The 7106-T63 and 7039-T6X31 alloys were relatively sensitive to SCC, while the 2219-T851 alloy was only slightly sensitive. Incompleted studies on several other alloys are in progress.

The long times required to establish the K_{Isc} threshold value for the sensitive alloys indicate that more accurate data maybe possible if the method of continuous replenishment of the salt water solution is utilized. However K_{Isc} values above those shown would not be expected.

HEAT-TREATMENT STUDIES (D.G. Howe)

Heat-treatment studies on a number of titanium alloys have been continued in order to determine whether selected vacuum heat treatments that have proven very beneficial to the stress-corrosion-cracking (SCC) resistance of the Ti-8Al-1Mo-1V and Ti-7Al-1Mo-1V alloy systems (4, 6, 22, 23) would be applicable to other alloy systems. The low interstitial alloys Ti-6Al-4V (T-27) and Ti-7Al-2.5Mo (T-94) were selected for part of this investigation as two alloys of particular interest for deep submersible applications.

Specimens of the Ti-6Al-4V (T-27) and Ti-7Al-2.5Mo (T-94) alloys were vacuum heat treated, followed by helium gas cooling and divided into three groups, set aside and exposed to laboratory atmospheric conditions for prescribed periods of time. These groups will be used to determine whether the beneficial effects shown possible by vacuum heat treatment were permanent or whether only a temporary non-susceptibility to attack by SCC had been obtained.

Group I vacuum heat-treated specimens were exposed to laboratory atmospheric conditions for two months prior to the cantilever beam SCC test. The results of the Group I tests are shown in Table 16. Groups II and III specimens heat treated at the same time as Group I are being exposed in a like manner and will be tested for SCC resistance six months and twelve months, respectively, after the vacuum heat treatment.

Group I tests show the Ti-6Al-4V and Ti-7Al-2.5Mo alloys have a very high resistance to attack by SCC two months after the vacuum heat treatment. The specimens that were aged at 1200°F for two hours and helium cooled picked up some contamination from the system during this operation. The variations in surface appearance after heat treatment are noted in Table 15. The test values however gave no indication of the contamination having much affect in the SCC behavior or the "dry" $K_{I\dot{x}}$ determinations.

The effect of vacuum and inert gas heat-treatment environments on the aqueous SCC resistance of the Ti-8Al-1Mo-1V (T-28) alloy in a 3.5 percent NaCl solution is shown in Table 17. The Charpy V energy values for the selected heat treatments are also presented in Table 16. The data for this alloy show that for solution annealing above the beta transus and possible subsequent aging a lowering of the fracture toughness can be expected.

TABLE 16

EFFECTS OF SEVERAL HEAT TREATMENTS ON THE RESISTANCE OF THE ALLOYS Ti-6Al-4V (T-27) AND Ti-7Al-2.5Mo (T-94) TO STRESS-CORROSION-CRACKING IN A 3.5 PERCENT NaCl SOLUTION

| Alloy No. | Nominal Composition | Solution Heat Treatment | Aging Heat Treatment | Appear. after H.F. No Break | KI (ksi/in) | Time (min) | K _{Isc} (ksi/in) | Time (Min) | K _{Ix} (ksi/in) | |
|-----------|---------------------|-----------------------------|-----------------------------|-----------------------------|-------------|------------|---------------------------|------------|--------------------------|-----------------------|
| | | | | | | | | | | As-received condition |
| T-27* | Ti-6Al-4V | As-received condition | | | | | 72 | 10 | | |
| | | 1700°F/1hr Vac/ Helium Cool | 1200°F/2hr Vac/ Helium Cool | gold color | 101 | 5 | 106 | 1 | 105 | |
| | | 1700°F/1hr Vac/ Helium Cool | 1200°F/2hr Vac/ Helium Cool | gold color | 110 | 5 | 113 | 2 | | |
| | | 1700°F/1hr Vac/ Helium Cool | ----- | bright and shiny | | | | | | |
| | | 1700°F/4hr Vac/ Helium Cool | 1200°F/2hr Vac/ Helium Cool | dark gray | | | | | 116 | |
| T-94** | Ti-7Al-2.5Mo | As-received condition | | | | | 76 | 60 | 81 | 1 |
| | | 1700°F/1hr Vac/ Helium Cool | 1200°F/2hr Vac/ Helium Cool | gold color | 92 | 5 | 95 | 2 | 109 | |
| | | 1700°F/1hr Vac/ Helium Cool | 1200°F/2hr Vac/ Helium Cool | gold color | 106 | 10 | 110 | 2 | | |
| | | 1700°F/1hr Vac/ Helium Cool | ----- | bright and shiny | | | | | | |
| | | 1700°F/4hr Vac/ Helium Cool | 1200°F/2hr Vac/ Helium Cool | dark gray | | | | | 114 | |

* T-27 Heat-treated specimens are Type B (1/2-in.x1-in.x5-in. with 1/32-in. side notch)
 ** T-94 Heat-treated specimens are Type C (1/2-in.x1 1/4-in.x5-in. with 1/32-in. side notch)

TABLE 17

EFFECT OF VACUUM AND INERT GAS HEAT TREATMENT ON AQUEOUS STRESS-CORROSION
CRACKING RESISTANCE OF THE ALLOY Ti-8Al-1Mo-1V (T-28) IN A 3.5% NaCl SOLUTION

| Specimen Type | Heat Treatment | K _I (ksi/in.) No Break | Time (Min.) | K _I sc (ksi/in.) Calcul. | Time To Break (Min.) | K _I A (ksi/in.) Calcul. Dry Break | Hydrogen Content (PPM) | Remarks | Cv (ft-lbs.) |
|---------------|--|---|----------------|---|----------------------------|---|------------------------------|---|-----------------|
| B | 1950°F/vacuum/2 hr/ helium cool in a "cold wall" furnace --No age-- | 118.2 110.1 | 10 450 | 121.2 117.4 | 5 2 | 121.2 117.4 | 17 Avg. | Non-susceptible to stress cor- rosion crack- ing | 47 Avg. |
| B | 1700°F/argon atm./ 1 hr/air cool 1200°F/argon atm./ 2 hr/water quench | 94.6 | 10 | 96.3 | 2 | | 20 | Slight suscep- tibility to stress corrosion cracking | 51 |
| B | 1950°F/argon atm./ 1 hr/air cool 1200°F/argon atm./ 2 hr/water quench | 40.3 | 10 | 43.7 | 5 | | 52 | VERY suscep- tible to stress corrosion cracking | 36 |

NOTE: All specimens are in the longitudinal direction (RW).
Beta transus for this material is 1885°F ± 15°F.

REFERENCES

1. Pellini, W.S., et al., "Review of Concepts and Status of Procedures for Fracture-Safe Design of Complex Welded Structures Involving Metals of Low to Ultra-High Strength Levels," NRL Report 6300, June 1965
2. Puzak, P.P., et al., "Metallurgical Characteristics of High Strength Structural Materials (Eighth Quarterly Report)," NRL Report 6364, August 1965
3. Goode, R.J., et al., "Metallurgical Characteristics of High Strength Structural Materials (Seventh Quarterly Report)," NRL Report 6327, May 1965
4. Goode, R.J., et al., "Metallurgical Characteristics of High Strength Structural Materials (Tenth Quarterly Report)," NRL Report 6454, April 1966 (publication pending)
5. McCaffrey, T.J. and Hiller, A.J., Technical Report, "Joint Research and Development Program 18% Nickel Maraging Steel (250 ksi)"
6. Goode, R.J., et al., "Metallurgical Characteristics of High Strength Structural Materials (Ninth Quarterly Report)," NRL Report 6405, November 1965
7. Goode, R.J., and Huber, R.W., "Fracture Toughness Characteristics of Some Titanium Alloys for Deep-Diving Vehicles," Journal of Metals, August 1965
8. The ASTM Committee on Fracture Testing of High-Strength Metallic Materials, "The Slow Growth and Rapid Propagation of Cracks" (Second Report), ASTM Materials Research Standards, Vol. 1, No. 5, May 1961
9. Symposium on Line Pipe Research presented by the Pipeline Research Committee of American Gas Association in Dallas, Texas, November 17-18, 1965
10. Sullivan, A.M., "New Specimen Design for Plane-Strain Fracture Toughness Tests," Materials Research & Standards, Vol. 4, No. 1, January 1964

11. Srawley, J. and Brown, W., "Fracture Toughness Testing," Lewis Research Center, Cleveland, Ohio, NASA TN D-2599, January 1965
12. Puzak, P.P., et al., "Metallurgical Characteristics of High Strength Structural Materials," NRL Report 6086, January 1964
13. Goode, R.J., et al., "Metallurgical Characteristics of High Strength Structural Materials (Fourth Quarterly Report)," NRL Report 6137, June 1964
14. Crooker, T.W., et al., "Metallurgical Characteristics of High Strength Structural Materials (Fifth Quarterly Report)," NRL Report 6196, September 1964
15. Pellini, W.S., et al., "Metallurgical Characteristics of High Strength Structural Materials (Sixth Quarterly Report)," NRL Report 6258, December 1964
16. Crooker, T.W., Morey, R.E., and Lange, E.A., "Low Cycle Fatigue Crack Propagation Characteristics of Monel 400 and Konel K-500 Alloys," NRL Report 6218, March 10, 1965
17. Crooker, T.W., Morey, R.E., and Lange, E.A., "Low Cycle Fatigue Crack Propagation, " Report of NRL Progress, June 1964, pp. 30-33
18. Crooker, T.W., Morey, R.E., and Lange, E.A., "Low Cycle Fatigue Crack Propagation," Report of NRL Progress, June 1965, pp. 37-40
19. Carman, C.M., and Katlin, J.M., "Low Cycle Fatigue Crack Propagation Characteristics of High-Strength Steels," ASME Paper No. 66-MET-3 (to be published in TRANSACTIONS ASME - J. Basic Engineering)
20. Brown, B.F., et al., "Marine Corrosion Studies (Third Interim Report of Progress)," NRL Memo Report 1634, July 1965
21. Brown, B.F., and Beachem, C.D., "A Study of the Stress Factor in Corrosion Cracking by Use of the Pre-Cracked Cantilever Beam Specimen," Corrosion Science, Vol. 5, 1965, pp. 745-750

22. Howe, D.G., "Effects of Heat Treatment on the Stress-Corrosion-Cracking Resistance of Several Ti-Al-Mo-V Alloys," Report of NRL Progress, February 1966, pp. 14-18
23. Howe, D.G., "Effects of Heat Treatment on the Stress-Corrosion-Cracking Resistance of Several Titanium Alloys," Report of NRL Progress, July 1966 (publication pending)

This page intentionally left blank.

DOCUMENT CONTROL DATA - R & D

(Security classification of title, body of abstract and indexing annotation must be entered when the overall report is classified)

| | | | |
|---|--|---|-----------------------|
| 1. ORIGINATING ACTIVITY (Corporate author) Naval Research Laboratory Washington, D.C. 20390 | | 2a. REPORT SECURITY CLASSIFICATION Unclassified | |
| | | 2b. GROUP | |
| 3. REPORT TITLE METALLURGICAL CHARACTERISTICS OF HIGH STRENGTH STRUCTURAL MATERIALS (Eleventh Quarterly Report) | | | |
| 4. DESCRIPTIVE NOTES (Type of report and inclusive dates) Eleventh Quarterly progress report - April - June 1966 | | | |
| 5. AUTHOR(S) (First name, middle initial, last name) Puzak, P.P., Lloyd, K.B., Huber, R.W., Goode, R.J., Lange, E.A., Freed, C.N., Crooker, T.W., Judy, R.W., Jr., and Howe, D.G. | | | |
| 6. REPORT DATE August 1966 | | 7a. TOTAL NO. OF PAGES 91 | 7b. NO. OF REFS 23 |
| 8a. CONTRACT OR GRANT NO. NRL Problem Nos. F01-17 | | 9a. ORIGINATOR'S REPORT NUMBER(S) NRL Report 6513 | |
| b. PROJECT NO. M01-05 | | | |
| c. M01-18 | | | |
| d. M03-01 M04-08B | | | |
| 9b. OTHER REPORT NO(S) (Any other numbers that may be assigned this report) | | | |
| 10. DISTRIBUTION STATEMENT Distribution of this report is unlimited. | | | |
| 11. SUPPLEMENTARY NOTES Copies available from CFSTI | | 12. SPONSORING MILITARY ACTIVITY Special Projects - Department of the Navy Office of Naval Research - Department of the Navy - ARPA - Department of Defense | |
| 13. ABSTRACT A progress report covering the research studies in high strength structural metals conducted during the period April through June 1966 is presented. The report includes fracture toughness studies on specially melted 18% Ni grade 250 ksi maraging steel and a Cr-Ni-Mo stainless steel. Welding studies on a 12Ni-5Cr-3Mo maraging steel with 12Ni-3Cr-3Mo and 17Ni-2Co-3Mo filler metal wire are described with the problems associated with developing optimum properties in both plate and weldment being discussed. Results of fracture toughness studies on titanium alloys and aluminum alloys are presented in which engineering type tests and fracture mechanics techniques are employed. The fracture toughness index diagrams for steels and titanium are presented based upon the correlations developed with the engineering test methods. Preliminary fracture toughness correlation diagrams are presented for titanium alloys based upon fracture mechanics test methods. Results of a study on the low cycle fatigue crack propagation of a 9Ni-4Co-0.25C steel in air and salt water is discussed and compared to similar data obtained for other steels covering a spectrum of yield strengths. Stress-corrosion-cracking studies were conducted on titanium alloys, aluminum alloys, and steels. The stress-corrosion-cracking resistance of these alloys is presented in terms of the stress intensity (K_{Isc}) required to cause crack propagation to occur due to the influence of the environment. A double-pendulum type, shock-free, 2000 ft-lb impact machine has been designed to obtain fracture appearance, tear energy, and dynamic K_{Ic} information on high strength structural metals using a subsize tear type specimen. Design details of this new test tool are presented. | | | |

| 14. KEY WORDS | LINK A | | LINK B | | LINK C | |
|---|--------|----|--------|----|--------|----|
| | ROLE | WT | ROLE | WT | ROLE | WT |
| High-strength structural metals Research Fracture toughness studies 18% Ni grade steel Cr-Ni-Mo stainless steel Titanium alloys Aluminum alloys Fatigue crack propagating Stress corrosion cracking | | | | | | |